NASA-CR-195494

NASW-4435

A GLOBAL RANGE MILITARY TRANSPORT

IN-05-CR
204239
P. 103

THE OSTRICH

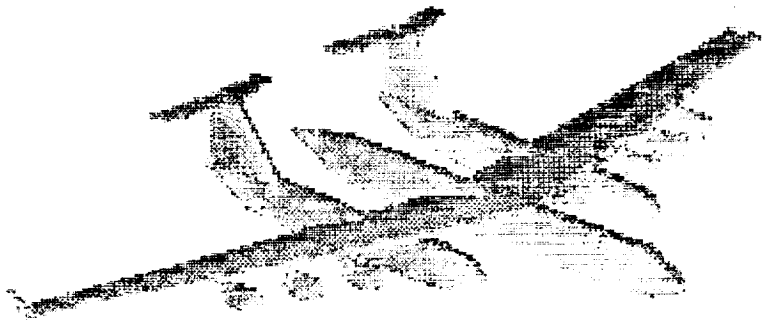

Team Members:

John Aguiar
Cecilia Booker
Eric Hoffman
James Kramar
Orlando Manahan
Ray Serranzana
Mike Taylor

Presented to:

Aeronautical Enginerering Department
California Polytechnic State University
San Luis Obispo, California
May 14, 1993

(NASA-CR-195494) A GLOBAL RANGE MILITARY TRANSPORT: THE OSTRICH (California Polytechnic State Univ.) 103 p

N94-24972

Unclas

G3/05 0204239

ABSTRACT

Studies have shown that there is an increasing need for a global range transport capable of carrying large numbers of troops and equipment to potential trouble spots throughout the world. The Ostrich is a solution to this problem. The Ostrich is capable of carrying 800,000 pounds, 6,500 n.m., and return with 15% payload, without refueling. With a technology availability date in 2010 and an initial operating capability of 2015 the aircraft incorporates many advanced technologies including laminar flow control, composite primary structures, and a unique multibody design.

By utilizing current technology, such as using McDonnell Douglas C-17 fuselage for the outer fuselages on the Ostrich, the cost for the aircraft was reduced. The cost of the Ostrich per aircraft is $ 1.2 billion with a direct operating cost of $56,000 per flight hour.

The Ostrich will provide a valuable service as a logistical transport capable of projecting a significant military force or humanitarian aid anywhere in the world rapidly.

TABLE OF CONTENTS

LIST OF TABLES

LIST OF FIGURES

Symbols

a.c.	Aerodynamic Center
ACN	Aircraft Classification Number
AEP	Aircraft Estimated Cost
APU	Auxiliary Power Unit
AR	Aspect Ratio
b	Wing span
c	chord
cj	Specific Fuel Consumption
CACQ	Acquisition Cost
c.g.	Center of Gravity
C_D	Drag coefficient
$C_{D_{L=0}}$	Zero lift drag coefficient
CDi	Induced drag coefficient
CDIS	Disposal Cost
CFD	Computational Fluid Dynamics
C_L	Total wing lift coefficient
C_{Lmax_L}	Maximum coefficient of lift at landing
C_{LmaxTO}	Maximum coefficient of lift at take-off
COP	Operating Cost
c_r	root chord
c_t	tip chord
e	Wing span efficiency
FAR	Federal Aviation Regulation
HUD	Head-Up Display
KEAS	Knots Equivalent Airspeed
Kts	Knots
L/D	Lift/Drag
LFC	Laminar Flow Control
M	Mach number
M_c	Cruise Mach number
MAC	Mean Aerodynamic Chord
max	Maximum
MFD	Multifunction Display
n	Load factor
n.m.	Nautical miles
OEI	One Engine Inoperative
OW	Operating weight
OWE	Operating weight empty
P_a	Power available
P_r	Power required
psf	Pounds per square foot

psi	Pounds per square inch
RDT&E	Research & Developement Test & Engineering
RFP	Request for proposal
S	Wing area
S_h	Horizontal tail area
S_v	Vertical tail area
SFC	Specific fuel consumption
S_{FL}	Field length distance
S_L	Landing distance
S_{LG}	Ground roll distance
SM	Static margin
S_{TOG}	Take-off ground roll distance
t/c	Thickness to chord ratio
TO	Take-off
V_A	Landing approach velocity
V_h	Horizontal tail volume coefficient
V_v	Vertical tail volume coefficient
V_s	Stall speed
V_{sl}	Stall speed with landing flaps
V_{LOF}	Lift off velocity
V_{STO}	Stall velocity at take-off
V_{TD}	Touchdown velocity
W_E	Empty Weight
WP	Payload Weight
W_{TO}	Take-off Weight
W/S	Wing loading

Stability Derivatives

C_{L_α}	Lift due to angle of attack derivative
C_{M_α}	Pitching moment due to angle of attack derivative
C_{M_α}	Pitching moment due to rate of angle of attack derivative
C_{M_q}	Pitching moment due to pitch rate derivative
$C_{M_{\delta e}}$	Pitching moment due to elevator derivative
$C_{L_{\delta e}}$	Lift due to elevator derivative
C_{Mi_H}	Pitching moment due to stabalizer incidence derivative
C_{Li_H}	Lift due to stabalizer incidence derivative
C_{n_β}	Yawing moment due to sideslip derivative
C_{l_β}	Rollintg moment due to sideslip derivative

Cy_{β}	Sideforce due to sideslip derivative
Cn_{p}	Yawing moment due to roll rate derivative
Cl_{p}	Rolling moment due to roll rate derivative
Cy_{p}	Sideforce due to roll rate derivative
Cn_{r}	Yawing moment due to yaw rate derivative
Cl_{r}	Rolling moment due to yaw rate derivative
Cy_{r}	Sideforce due to yaw rate derivative
$Cn_{\delta r}$	Sideforce due to rudder derivative
$Cl_{\delta r}$	Rolling moment due to rudder derivative
$Cy_{\delta r}$	Yawing moment due to rudder derivative
$Cn_{\delta a}$	Yawing moment due to aileron derivative
$Cl_{\delta a}$	Rolling moment due to aileron derivative

1.0 INTRODUCTION

The world is rapidly changing from one where there are two primary military superpowers, to a world with many smaller military powers. The United States cannot depend on the availability of over sea bases from which to respond to crises requiring military intervention or humanitarian aid. Studies, including the SAB Global Reach and the Global Power Study, have confirmed this increased need to be able to rapidly transport large numbers of troops and equipment from the continental United States to potential trouble spots in the world (Ref. 1).

The following report outlines the concept design and justification for a transport aircraft capable of transporting large numbers of troops and equipment. Given an R.F.P., the objective was to design a global range transport aircraft, incorporating advanced technologies, capable of operating from existing military and commercial facilities. The technology availability date is 2010 with a planned initial operational capability by 2015. The aircraft had to meet all applicable military specifications as well as FAR 25 requirements (such as noise restrictions) that would limit conversion to civil applications (Ref. 1).

Figure 1.1 shows a possible solution to the problems that we may soon be facing: The Ostrich.

1.1 Existing Aircraft

The primary aircraft currently being used for long range transport include the Lockheed C-130 and C-5, and the McDonnell Douglas C-17. They are limited, however, by range and payload. The range requirement for the Ostrich is over five times that of the C-130 and the C-17, and three

FOLDOUT FRAME 1

THE OSTRICH

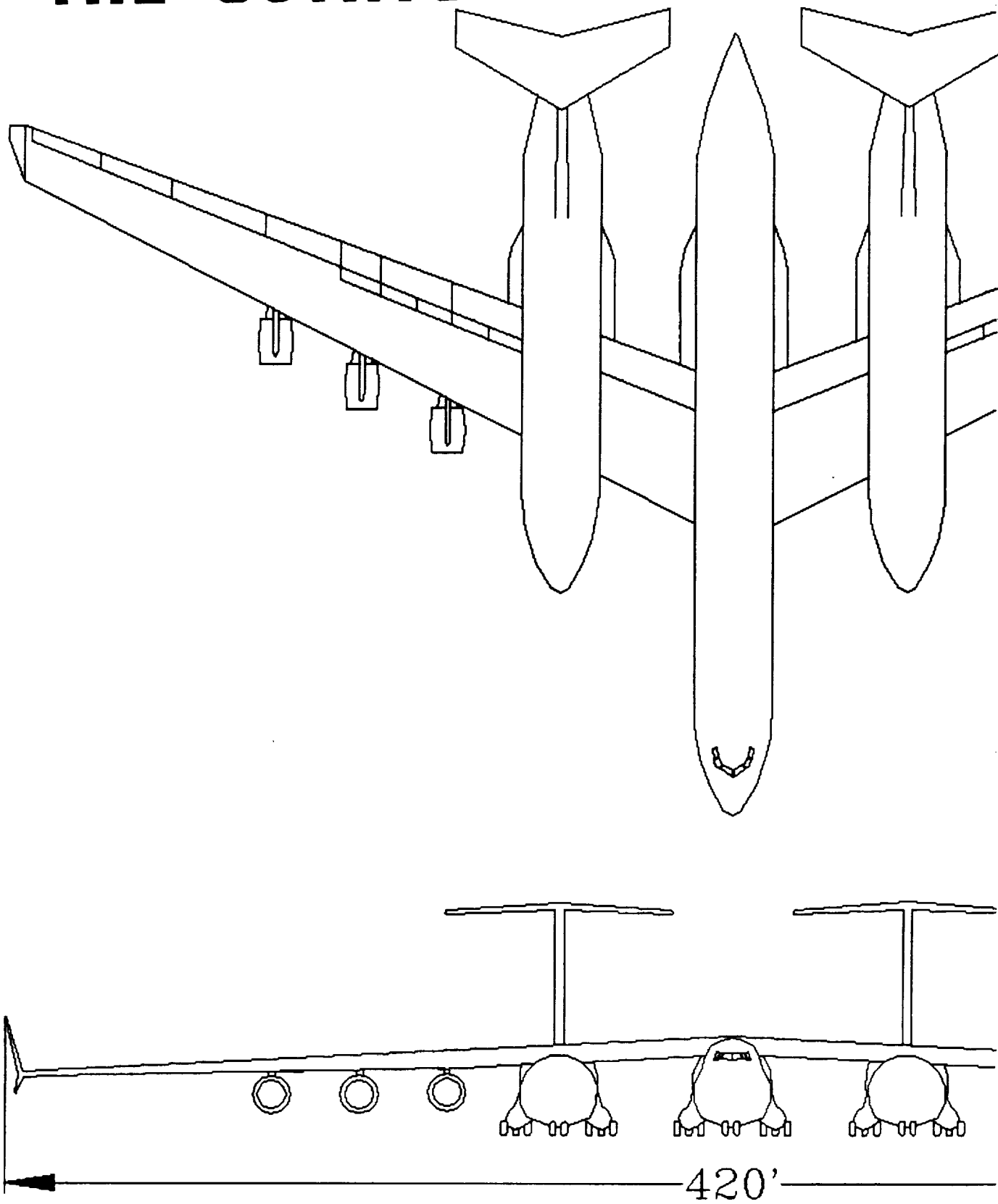

Figure 1.1 Three View of The Ostrich

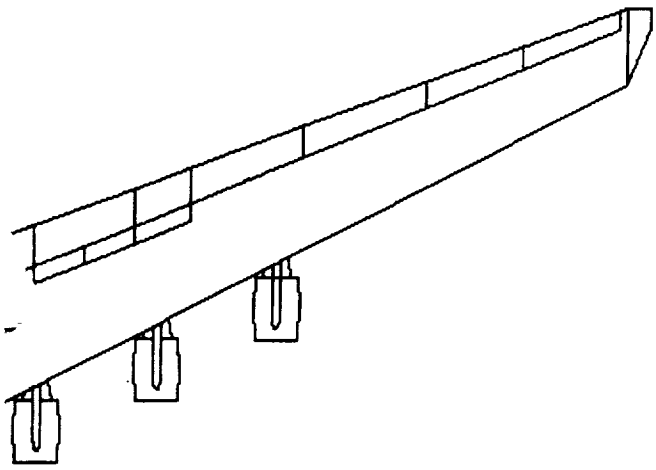

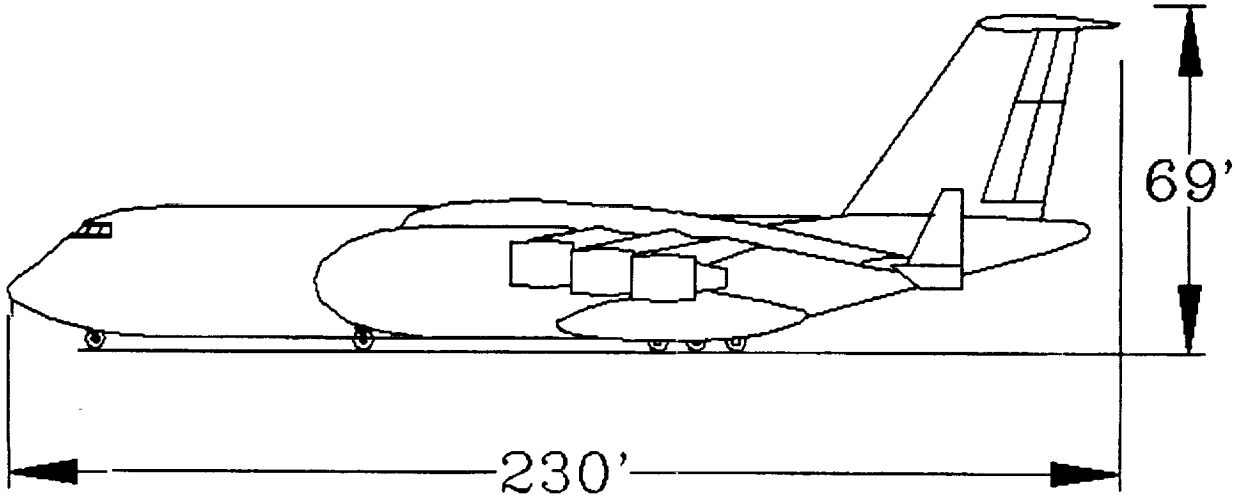
69'
230'

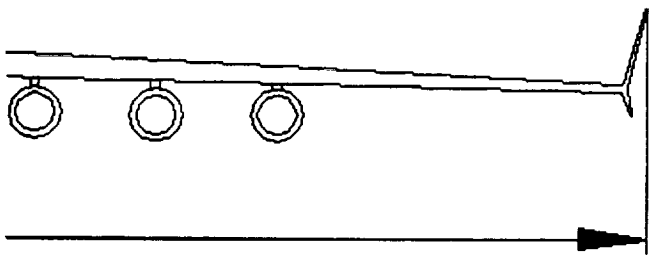

and a half times the range of the C-5. The payload requirement is three times that of the C-5, four and one half times that of the C-17, and twenty-one times that of the C-130 (Ref. 17). This is illustrated in Figure 1.2. The greatest improvement in the Ostrich is the increased range.

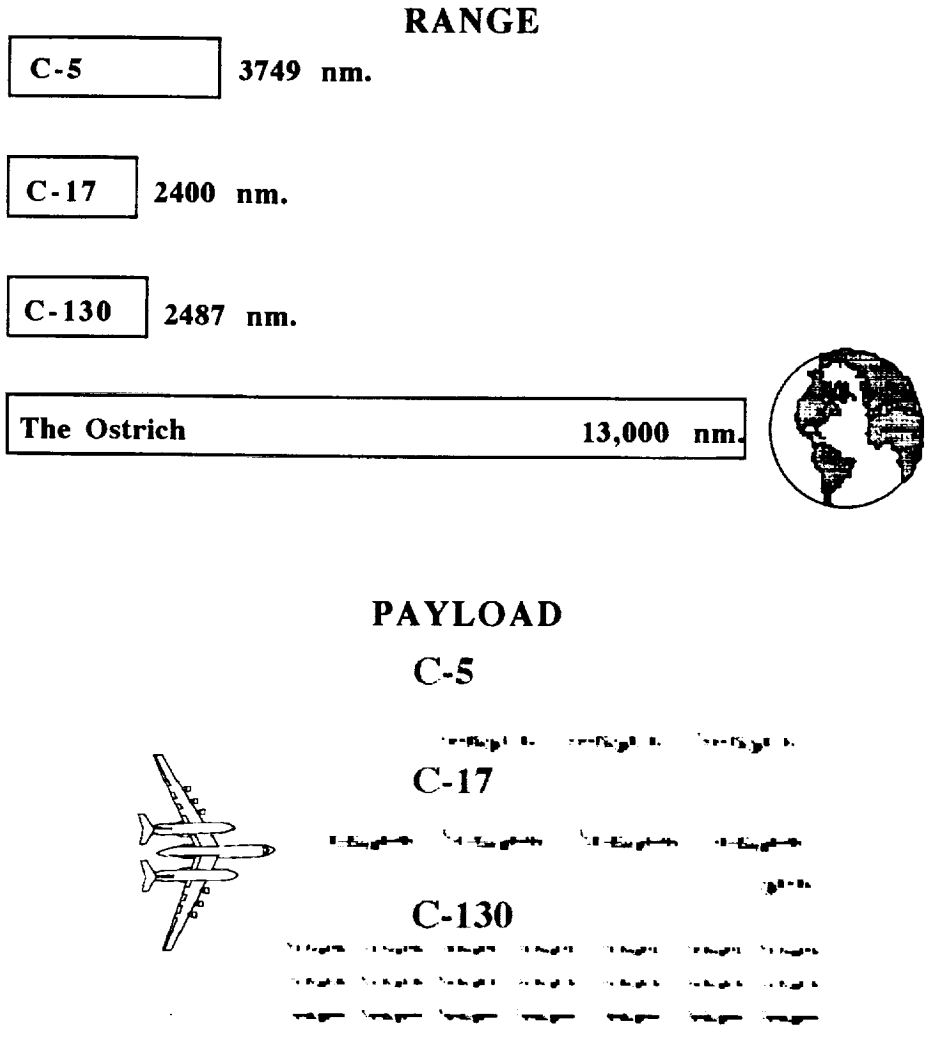

Figure 1.2 Range and Payload Comparison for The Ostrich

1.2 Concept Development

Two main factors guided the design of the Ostrich. The first was a need to keep the size to a minimum. The aircraft had to be unusually large to handle the payload and range requirements, but still had to be able to utilize existing facilities. This meant keeping the wing span as small as possible.

The other factor, which was just as important, was the cost. With cuts in military spending, the cost of new developments needs to be kept as low as possible. By using existing technologies and existing McDonnell Douglas C-17 fuselages, with slight modifications, in the design of the Ostrich, the cost was dramatically reduced.

2.0 MISSION REQUIREMENTS

The primary mission for this aircraft is to carry a 800,000 pound payload 6,500 n.m., off load, and return with 15% of the full payload, without refueling. A secondary mission may be to fly 8,000 to 12,000 n.m. with at least 75% payload, land and return empty, without refueling.

A typical payload for this aircraft may include six M-1 tanks, three AH-1G helicopters, twenty 463L pallets, and 200 troops (Ref. 1). Although the Ostrich can hold this volume, the sample payload listed is actually well above 800,000 pounds.

The Ostrich will perform missions similar to current military transports, but with a much greater range and payload. The mission profile will consist of the following (Ref. 1):

1. Engine warm-up and taxi for 15 minutes.
2. Takeoff and climb to 35,000 ft.
3. Cruise at Mach 0.73 for 6,500 n.m.
4. Descend on course and land.
5. Taxi and idle for 30 minutes, off load full payload.
6. Load 15% of full payload, takeoff and climb to 35,000 ft.
7. Cruise at Mach 0.73 for 6,500 n.m.
8. Loiter 15 minutes.
9. Descend, land and taxi 10 minutes.

The mission profile is shown in Figure 2.1.

The initial airfield critical field length is 10,000 feet at sea level standard day and the midpoint airfield critical field length is no more than 8,000 feet at 4,000 ft. elevation and 95°F.

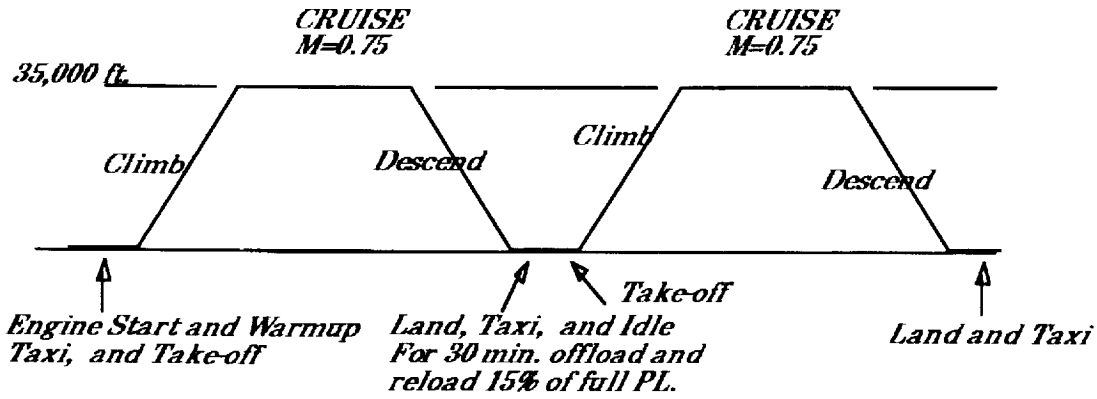

Initial Airfield Critical Length = 10,000ft @ SeaLevel Std Day
Midpoint Airfield Critical Field Length < 8,000ft @ 4,000ft alt.

Figure 2.1 Mission Profile for The Ostrich

3.0 PRELIMINARY SIZING

3.1 Weight Sizing

In order to complete the preliminary design of the Ostrich, the mission specifications were combined with a class one sizing method from Reference 19. To calculate the aircraft parameters such as gross weight, fuel weight and empty weight, the fuel fraction method was used in conjunction with the specifications given in Reference 1. The performance parameters of the aircraft were estimated from empirical data. The results of the preliminary sizing process are given in Table 3.1. These numbers show that the gross takeoff weight of the Ostrich is six times the gross weight of Lockheed's C-5B.

Table 3.1 Weight Sizing Results for the Ostrich

WEIGHTS	POUNDS
Payload weight	800,000
Mission fuel weight	839,000
Operating empty weight	650,000
Trapped fuel/oil weight	5,000
Crew weight (6 crew)	1,200
Empty weight	640,000
Fuel fraction (ff)	0.61
Gross take-off weight	2.3 million

3.2 Performance Sizing

After estimating a preliminary weight, the next step was to determine the best thrust-to-weight ratio (T/W) and wing loading (W/S). This was done by establishing a series of relations between T/W, W/S, maximum required lift coefficient (C_{Lmax}) and aspect ratio (AR). The

design point was obtained by combining and graphing these relations as shown in Figure 3.1 and is explained in the following subsections.

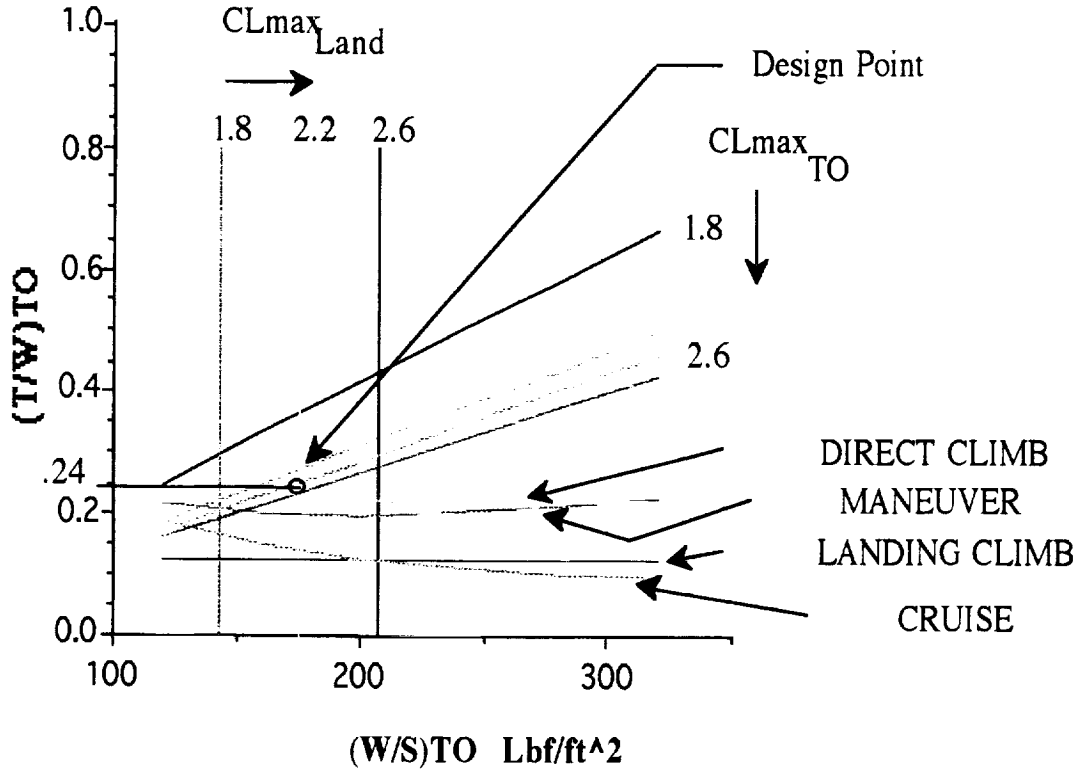

Figure 3.1 Design Point for the Ostrich

3.2.1 Aircraft Take-off Sizing

In order to size the Ostrich for takeoff requirements (Ref. 19), the take-off weight, speed, T/W and W/S were used with the takeoff field length restrictions to determine the lift coefficient at take-off (C_{LmaxTO}). The required C_{LmaxTO} was calculated to be 2.6. Because the C_{LmaxTO} was so high, it was important to develop a low drag, high lift system for the take-off configuration.

3.2.2 Aircraft Landing Restriction

The coefficient of lift at landing, C_{LmaxL}, was determined using the relationship (Ref. 19) between W/S, landing weight, approach speed and critical field length. The C_{LmaxL} was established from the design point to be 2.2, but the aircraft was designed with a C_{LmaxL} of 3.2, in order to obtain a slower approach speed.

3.2.3 Maneuver and Cruise Requirement

The aircraft was sized for the cruise requirement at the design Mach number of 0.73 and flight altitude of 35,000 ft. The Mach number of 0.73 was used because it was the best balance between speed and wave drag. The maneuvering requirement was greatly dependent on the installed thrust, maximum lift coefficient and the load factor; the load factor of 2.5g's was specified in Reference 1. These requirements for cruise and maneuver were not critical in establishing the design point.

3.2.4 Direct Climb

For the direct climb sizing, it was required to be able to directly climb to an altitude of 35,000 ft at gross take-off weight, with a minimum required climb rate of 300 fpm (Ref. 19). The direct climb requirement was critical for determining the design point.

3.2.5 Matching Results

The design point, shown in Figure 3.1, was used to find a resulting design region. This graph is the result of the sizing requirements for the Ostrich. A low thrust-to-weight ratio and high wing loading was desired in order to obtain the lowest weight and the lowest cost possible. The design point was limited by the direct climb requirement and the high C_{LmaxTO}. The T/W and W/S were chosen to be 0.24 and 180 psf,

respectively. Table 3.2 summarizes the results of the design point and compares them to Lockheed's C-5B aircraft.

Table 3.2 Preliminary Design Results

PARAMETER	OSTRICH	C-5B
T/W	0.24	0.21
W/S	180 psf	135 psf
S_{ref}	12,500ft	6,400ft
AR	13	7.75
C_{LmaxL}	2.2	
C_{LmaxTO}	2.6	

3.3 Sensitivity Studies

After the preliminary sizing of the Ostrich, it was necessary to conduct sensitivity studies on the following parameters: range, specific fuel consumption (SFC), L/D and cruise speed. This was done in order to find out which parameters drive the design of the Ostrich. The results of the sensitivity studies are shown in Figures 3.2-3.5. The mission performance was kept the same when conducting these studies, using the following parameters:

- M = 0.73
- h = 35,000 ft
- R = 13,000 nm (Ref. 1)
- SFC = 0.4 (obtained from Fig. 5.1)
- L/D = 24 (obtained from preliminary sizing)
- W_{TO} = 2.3 million lbs (from preliminary sizing)

Figure 3.2 shows that as the SFC is increased, the take-off weight increases. A SFC of 0.4 was used for the preliminary sizing. If this

parameter were to increase by 0.05, the take-off weight would increase by 350,000 lbs. This figure also shows that by varying the altitude from 35,000 to 30,000 ft, $W_{T\,O}$ would increase by approximately 1%.

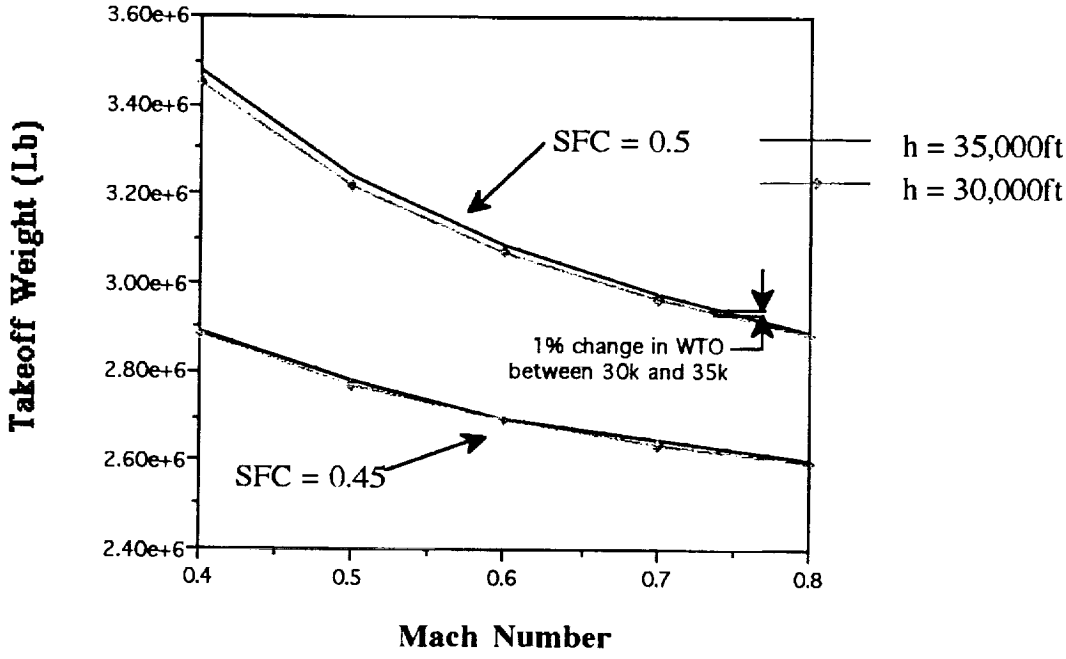

Figure 3.2 Sensitivities of Wto vs. SFC for the Ostrich

The sensitivities of take-off weight to the lift-to-drag ratio is shown in Figure 3.3. This figure varies L/D from 26 to 28. As L/D increases, W_{TO} decreases. The Ostrich was estimated to have a L/D of 24, but if this were to increase by 2, the take-off weight would decrease by about 250,000 lbs. If the Mach number were to decrease from 0.73 to 0.6, W_{TO} would decrease by 40,000 lbs. Again, a decrease in altitude did not make a difference.

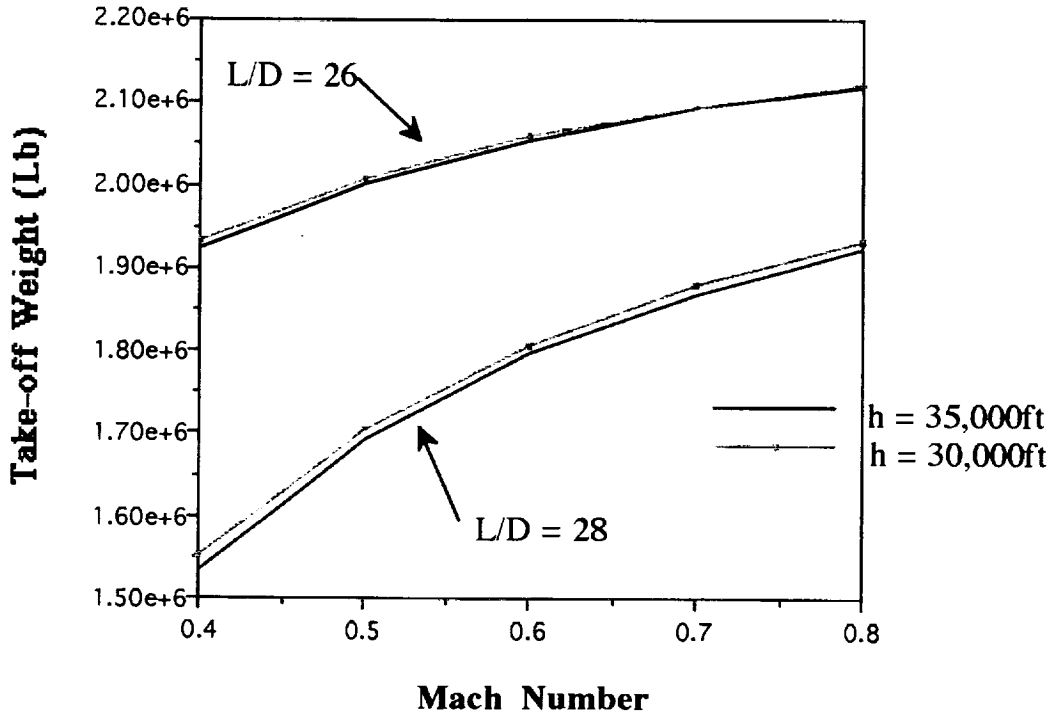

Figure 3.3 Sensitivities of Wto vs. L/D for the Ostrich

The growth factor due to range is equal to 196 lbs/nm. This means that if the range were to increase by 1,000 nm, the take-off weight would increase by 196,000 lbs as seen in Figure 3.4. Figure 3.5 shows that as you increase the Mach number, the take-off weight increases.

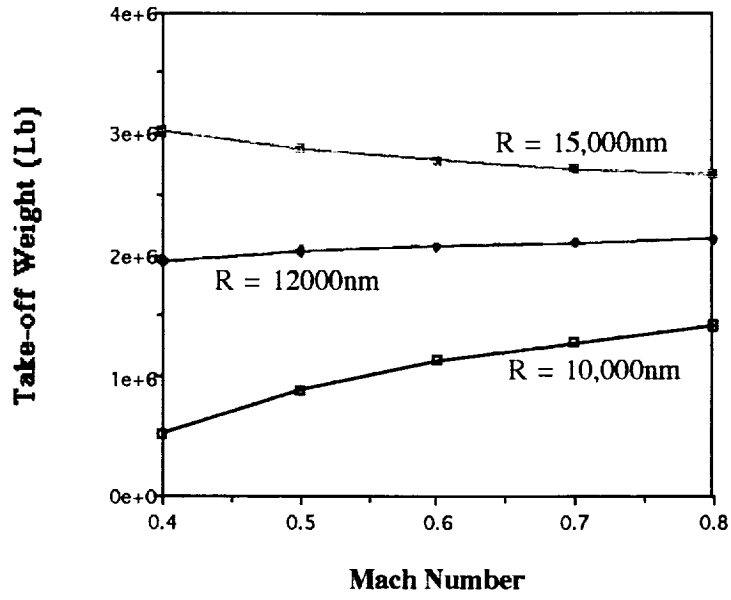

Figure 3.4 Sensitivities of Wto Range for the Ostrich

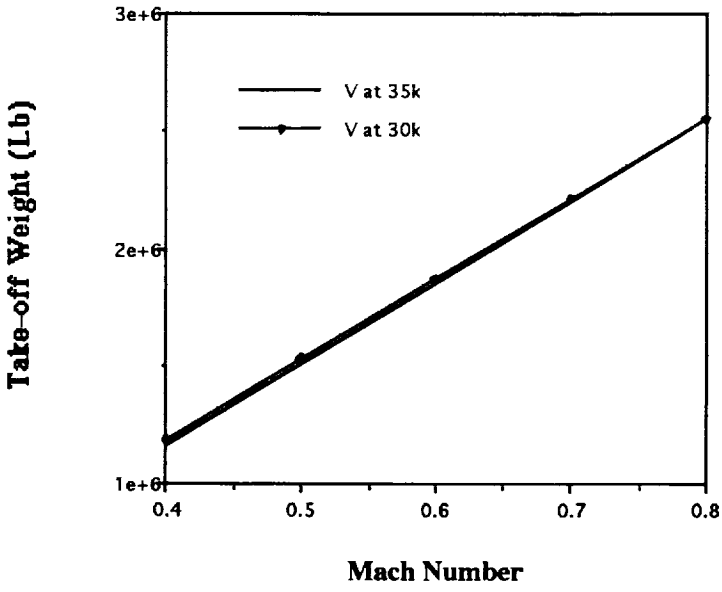

Figure 3.5 Sensitivities of Wto vs. Mach No. for the Ostrich

From the above sensitivity studies it was concluded that a low specific fuel consumption was necessary in order to keep the take-off weight as low as possible. Using Figure 3.2 and Figure 5.1, which gives future projectoins for SFC, a value of 0.4 was chosen. From Figure 3.5 it was found that the take-off weight increased with Mach number. The design Mach number of 0.73 was a compromise between speed and drag. The altitude originally assumed of 35,000 ft is not ideal, but from the sensitivity studies it does not seem to vary the performance parameters much.

4.0 CONFIGURATION

4.1 Aircraft Configuration

The configuration of the Ostrich aircraft was selected after the consideration of several different designs. Weight, aerodynamic efficiency, loadability and cost were the primary concerns in the selection of a configuration. The three body fuselage design was selected after comparing this design to other designs such as a flying wing and single fuselage.

Studies have shown that a multibody aircraft configuration offers many of the advantages of a span-distributed-load aircraft while retaining configurational and operational characteristics much like those of conventional transport aircraft. Reduced wing root bending moments and reduced costs were the main factors in choosing the multibody configuration concept. Reduced wing bending moment is accomplished by distributing the load along the wing. This in turn reduces the overall weight of the wing due to the reduction in the amount of structure required.

The overall cost of the multibody aircraft can be reduced by using existing fuselages instead of designing a single fuselage that is capable of handling this size payload. A further reduction in cost is obtained from part commonalty associated with the use of multiple fuselages and empennages.

Another consideration in choosing this configuration was the ability to load and unload the aircraft efficiently. The three-body configuration, because it has multiple cargo loading doors, offers reduced loading times and therefore minimizing turnaround times.

A two-body configuration would have advantages similar to the three-body configuration, such as effective span-loading and low turnaround time. However, a distinct disadvantage to a two-body design would be a significant reduction in ride quality during maneuvering because the location of the crew and troops would not be along the centerline of the aircraft. Also, existing fuselages could not be incorporated into the design, because of insufficient cargo capabilities.

4.2 Wing Design

4.2.1 Wing Configuration

The driving factors for wing design were high lift, low drag, stability and control considerations and low wing weight. The span was based on the initial sizing that took into account all of the performance requirements that were set forth in Reference 1. Minimizing take-off weight was of great importance to the viability of this aircraft. The most feasible way of accomplishing this was to use a high L/D ratio in the initial sizing. In order to obtain a high L/D ratio a wing of enormous span is necessary. An aspect ratio of 13 was chosen to reduce the induced drag produced by the wing. However, it must be noted that this is an aerodynamic aspect ratio, not a structural aspect ratio. Our structural aspect ratio is only 10, because of the outer fuselages acting as a support for the wing. A total wing area of 12,500 sq. ft. was needed to produce the necessary lift for the Ostrich. This resulted in a wingspan of 420 ft. The wing is set at 3 degree incidence at the fuselage to achieve the needed amount of lift during cruise conditions. A taper ratio of 0.35 was used to obtain the correct balance in structural and aerodynamic qualities. The sweep was set at 25 degrees at the quarter chord position to delay drag

divergence during normal flight operations. Because of the enormous size of the wing, it was found that there is plenty of room for fuel.

The wing dimensions are summarized in Table 4.1. A detailed drawing of the wing is shown in Figure 4.1.

Table 4.1 Wing Dimensions

Span	420 ft
Wing Area	12,500 sq. ft.
AR	13
Sweep @c/4	25°
Taper Ratio	0.35

Winglets were placed on the wing tips to lessen the effects of induced drag. The design considerations for the winglets were taken from a NASA study (Ref. 13). Reference 22 suggested that the top winglet to be set at a height equal to the tip chord of the main wing, which is 16 ft. The reference also stated that the taper ratio and the sweep of the upper winglet should be kept the same as that of the main wing. This basic configuration will ensure elliptical load distributions. To make sure that the upper winglet did not interfere with the oncoming flow, it was set back about 0.50c from the leading edge of the wing. The lower winglet was put on the leading edge of the airfoil to help with pressure recovery at the trailing edge of the wing. The lower winglet span was set at about $0.20c_t$ to allow for sufficient ground clearance. The general findings, in Reference 22, of correctly designed winglets is a 15% reduction in C_{Di} during cruise conditions. Further refinements may be accomplished by the use of wind tunnel studies and computational fluid dynamics (CFD). The details are shown in Figure 4.2.

THE OSTRICH

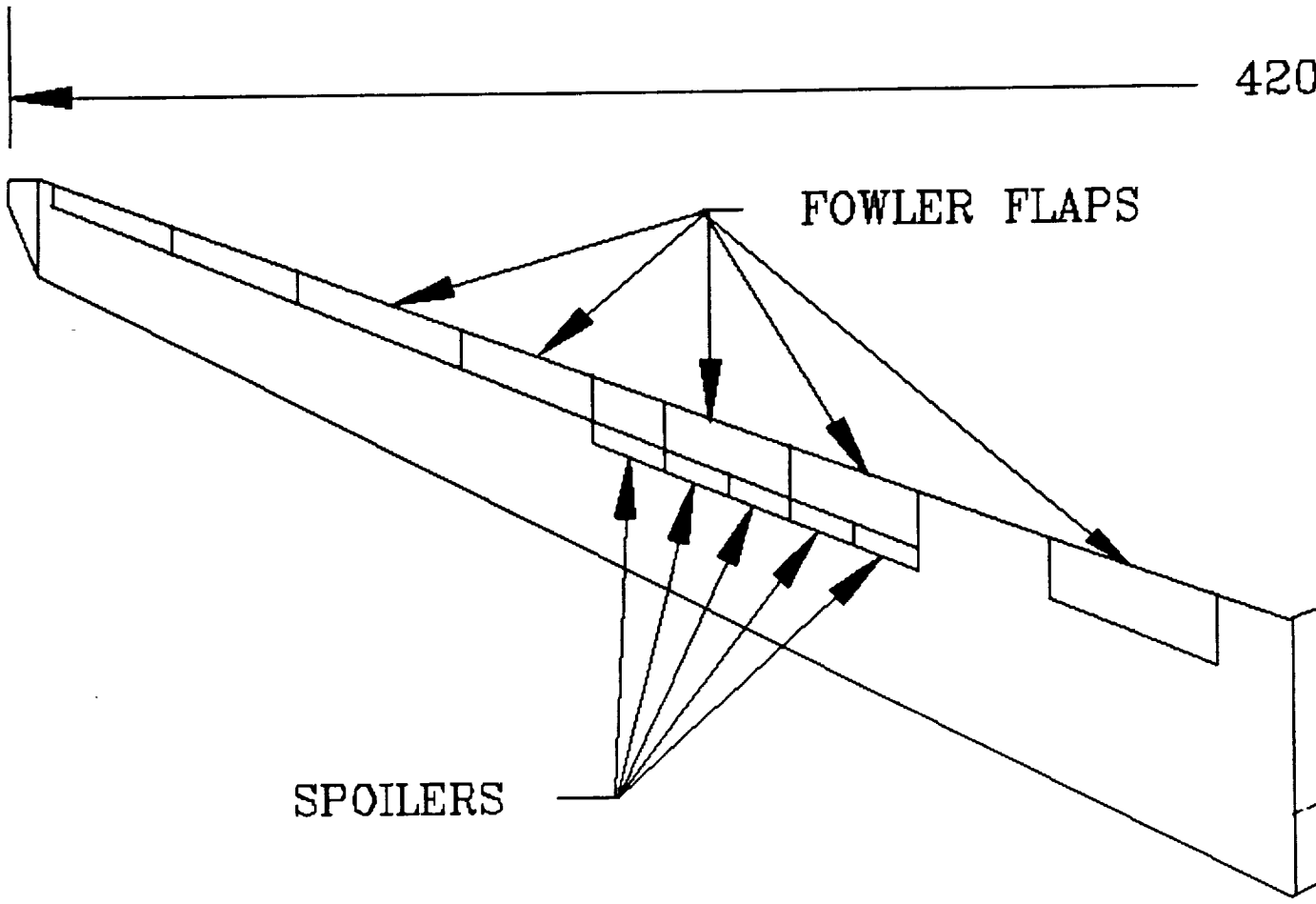

Figure 4.1 Wing Detail for The Ostrich

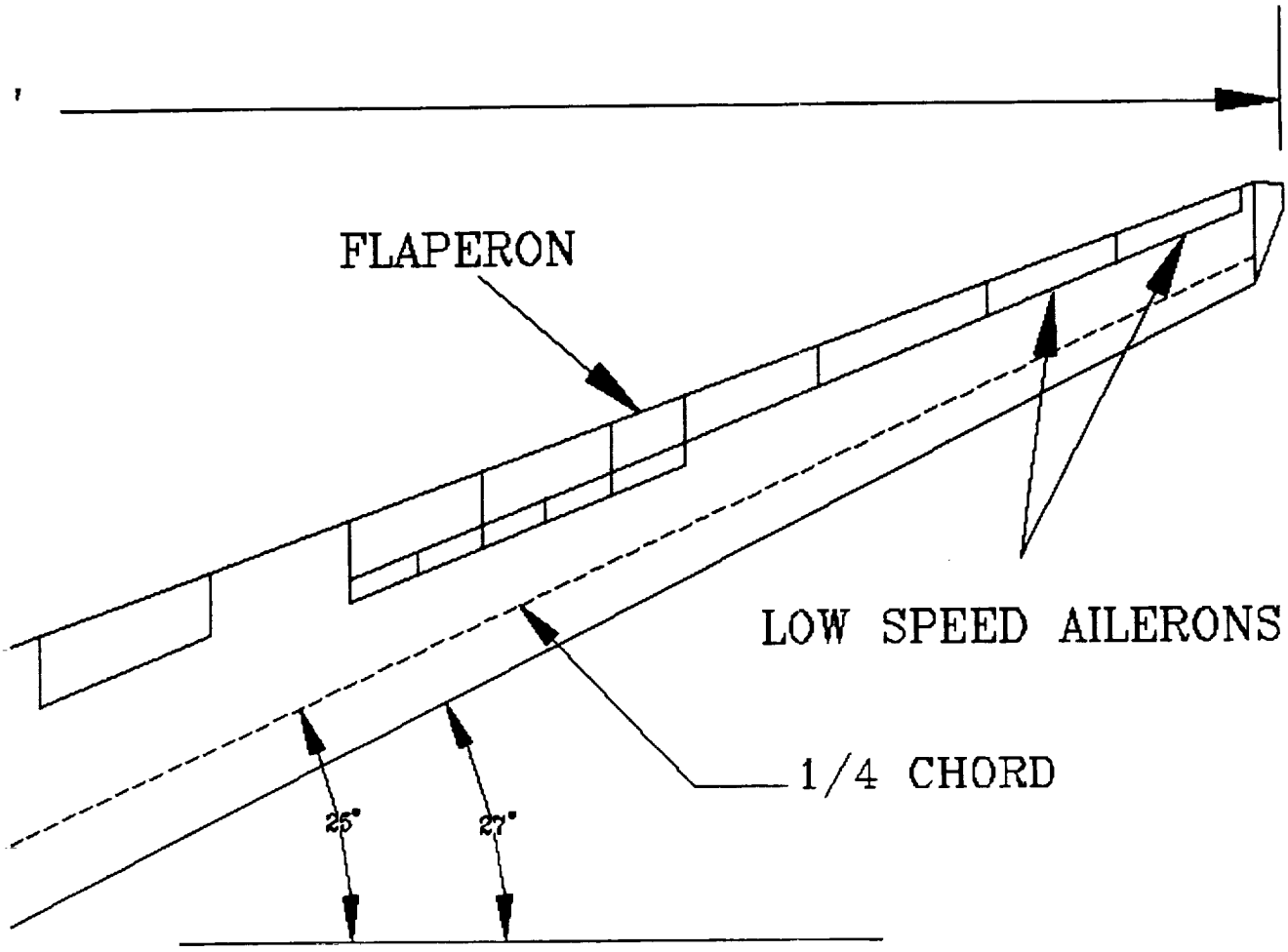
FLAPERON
LOW SPEED AILERONS
1/4 CHORD
25°
27°

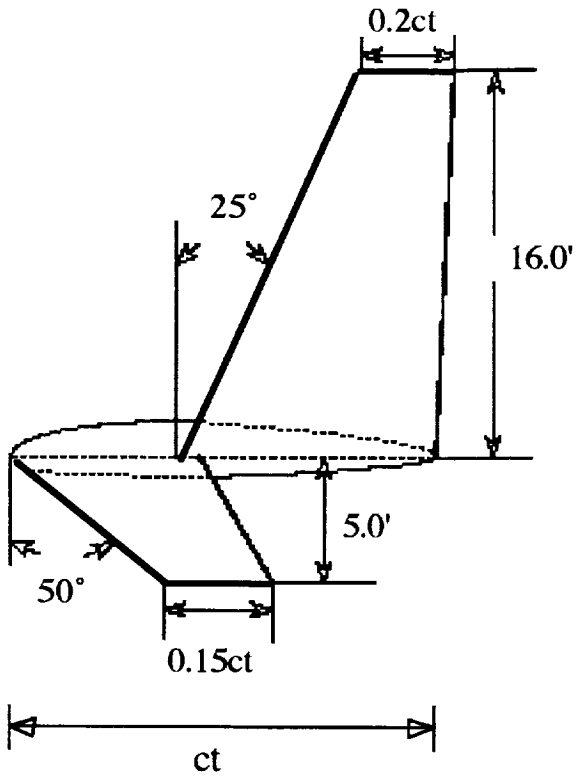

Figure 4.2 Winglet Dimensions for the Ostrich

Fowler flaps were used at the trailing edge of the wing to obtain high lift at take-off and landing. Fowler flaps were found to be the most efficient type of flaps. The flaps run 80% span and with a flap chord ratio of 0.30. The flaps are deployed at 15 degree and 30 degree deflections for take-off and landing respectively.

Laminar Flow Control (LFC) suction capability is used on the leading edge and top of the wing. LFC is implemented to increase the L/D by sucking the shear layer through a porous titanium skin, and therefore increasing lift and reducing the skin friction drag by delaying transition. The LFC will run full span and up to 70% of the wing chord.

4.2.2 Airfoil Selection

The airfoil selection for the Ostrich was a derivative of the supercritical MS-86 airfoil (Ref. 3). By comparing several airfoils it was found that the supercritical MS-86 most closely matched the requirements of the Ostrich during cruise. The MS-86 has a C_L of 0.65 at an angle of attack of one degree. In order to obtain the desired lift distribution along the span several derivatives of this airfoil would be obtained using transonic airfoil codes.

4.2.3 Laminar Flow Control

The use of LFC has been found to be a significant development in the aerodynamics field. From studies, Reference 11, that have been published about the use of LFC, projections are that by the year 2010, which is the technology availability date for the Ostrich, LFC will produce a 20% increase in L/D. This, in return, can lower the take-off weight of the aircraft because of the reduction in the amount of fuel that must be carried.

The implementation of LFC does require a certain amount of equipment, but that weight is easily offset by the reduction in the amount of fuel required. The LFC consists of a titanium skin placed on the leading edge and top surface of the wing. Titanium was chosen because of its hardness and low coefficient of thermal expansion which ensures the integrity of the holes used in the LFC system. The holes are machined such that the diameter of the holes decrease as they approach the surface of the titanium skin. This is to reduce clogging. To keep the skin clean, the suction pumps are able to blow a glycol solution outwards through the holes which coats the leading edge. This is done prior to take-off to clear

the holes and create a slick surface that prevents insects from sticking. A weight breakdown for the system is shown in Figure 4.3.

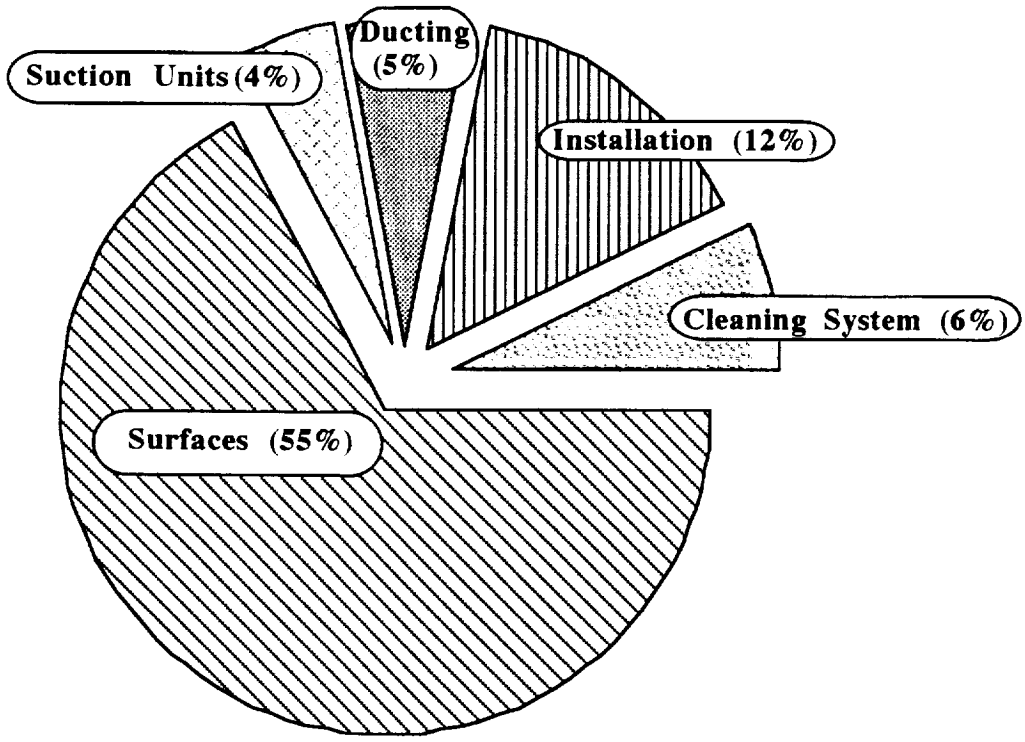

Figure 4.3 LFC Weight Breakdown for the Ostrich

4.3 Fuselage Design

4.3.1 Fuselage Configuration

The design of the fuselage was driven by three primary factors: payload capability, weight, and cost. The best compromise was obtained by using an existing fuselage for the outboard fuselages on the Ostrich. The fuselage chosen was the McDonnell Douglas C-17 because it is a relatively new aircraft which utilizes new technology and which is capable of carrying oversized loads as required by Reference 1. The center fuselage required seating for 200 troops and a greater cargo capacity than

the McDonnell Douglas C-17 could provide. However, many of the same components that are used on the outside fuselages are also utilized on the inside fuselage. These parts include the loading ramp, cargo door, cargo floor, gear systems and loadmaster stations.

Because of the multibody configuration, fuselage placement was of great importance. The outer fuselage spanwise location was chosen after considering several tradeoffs. In order to obtain a maximum reduction in the wing bending moment it is desirable to place the fuselages as close to the 39% semi-span position as possible (Ref 14). However, placing fuselages this far apart seriously reduces the number of runways from which the aircraft can operate due to the wide spacing of the landing gear. Large runways typically range from 150 ft. to 200 ft. in width. With a fuselage placement at 39% semispan, the Ostrich would have only about two feet of clearance between the landing gear and the edge of a 200 ft. wide runway. In addition to this, maneuverability is significantly reduced for the same amount of control power.(Ref 15) A compromise was made with an outer fuselage spacing of 100 feet from centerline to centerline (23% semi-span), which gives the Ostrich about ten feet of clearance between the landing gear and the edge of a 150 ft. wide runway.

4.3.2 Interior Configuration

4.3.2.1 Troop Seating Accommodations for 200 troops are provided on the upper deck of the center fuselage. There are a total of four lavatories, two forward of the wing box and two aft of the wing box. Stairs to the cargo bay in the center fuselage are located directly behind the wing box and in the crew rest area, allowing access between the forward and aft sections of the upper deck which is separated by the wing box.

There are a total of eight emergency exits, four forward of the wing box and four aft of the wing box. Each exit is equipped with an inflatable emergency slide.

The troop seating area was designed to seat the required 200 troops as compactly as possible while still maintaining a satisfactory amount of comfort keeping in mind the possibility of very long flights. Troop seats with a 20 inch width and 32 inch seat pitch were arranged six abreast with a 20 inch aisle down the center. An aisle height of 80 inches allows sufficient headroom. Overhead bins as well as under seat space are provided for gear storage. The cross section of the center fuselage is shown in Figure 4.4. The top view of the upper deck is shown in Figure 4.5.

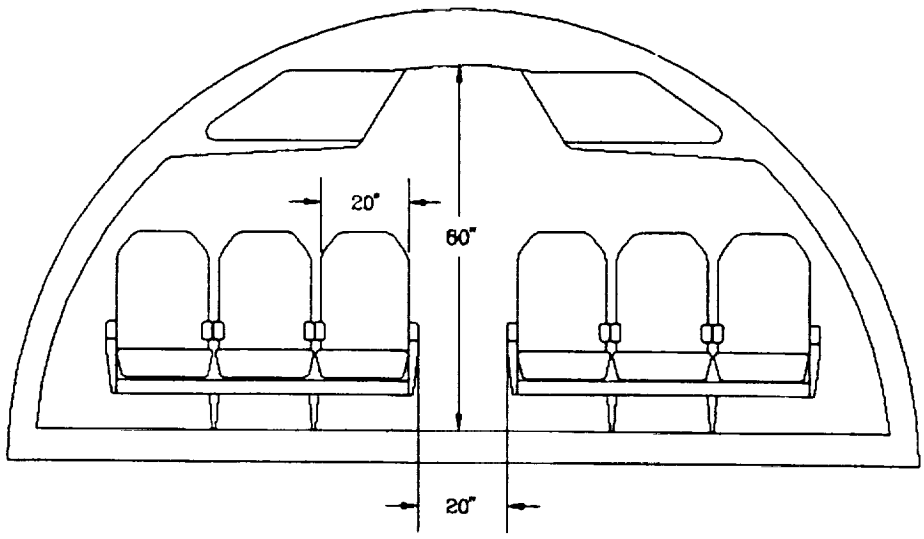

Figure 4.4 Upper Deck Cross Section for the Ostrich

FOLDOUT FRAME 1

THE OSTRICH

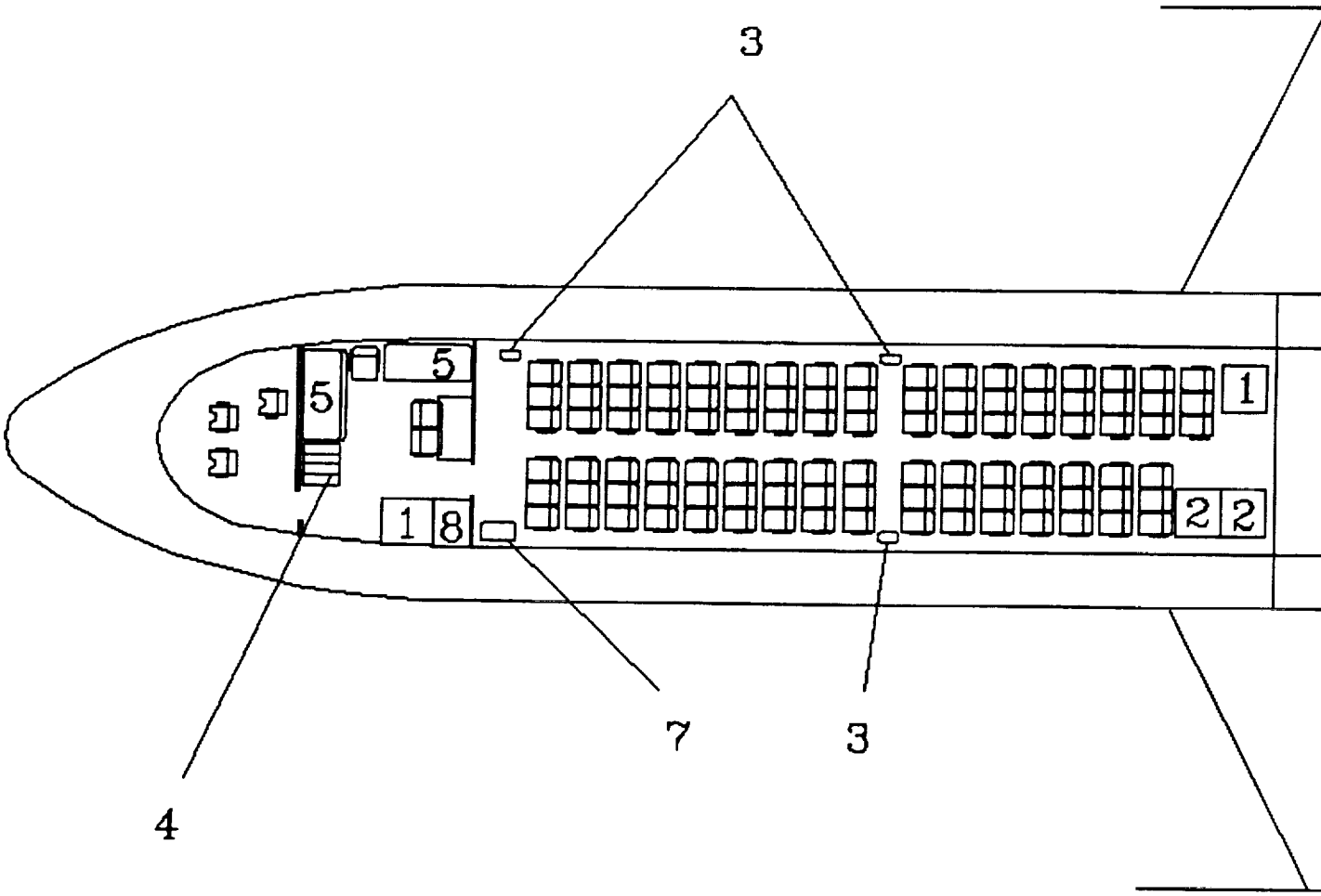

1 – GALLEYS
2 – LAVATORIES
3 – EMERGENCY EXITS
4 – STAIRS

Figure 4.5 Upper Deck Top View for The Ostrich

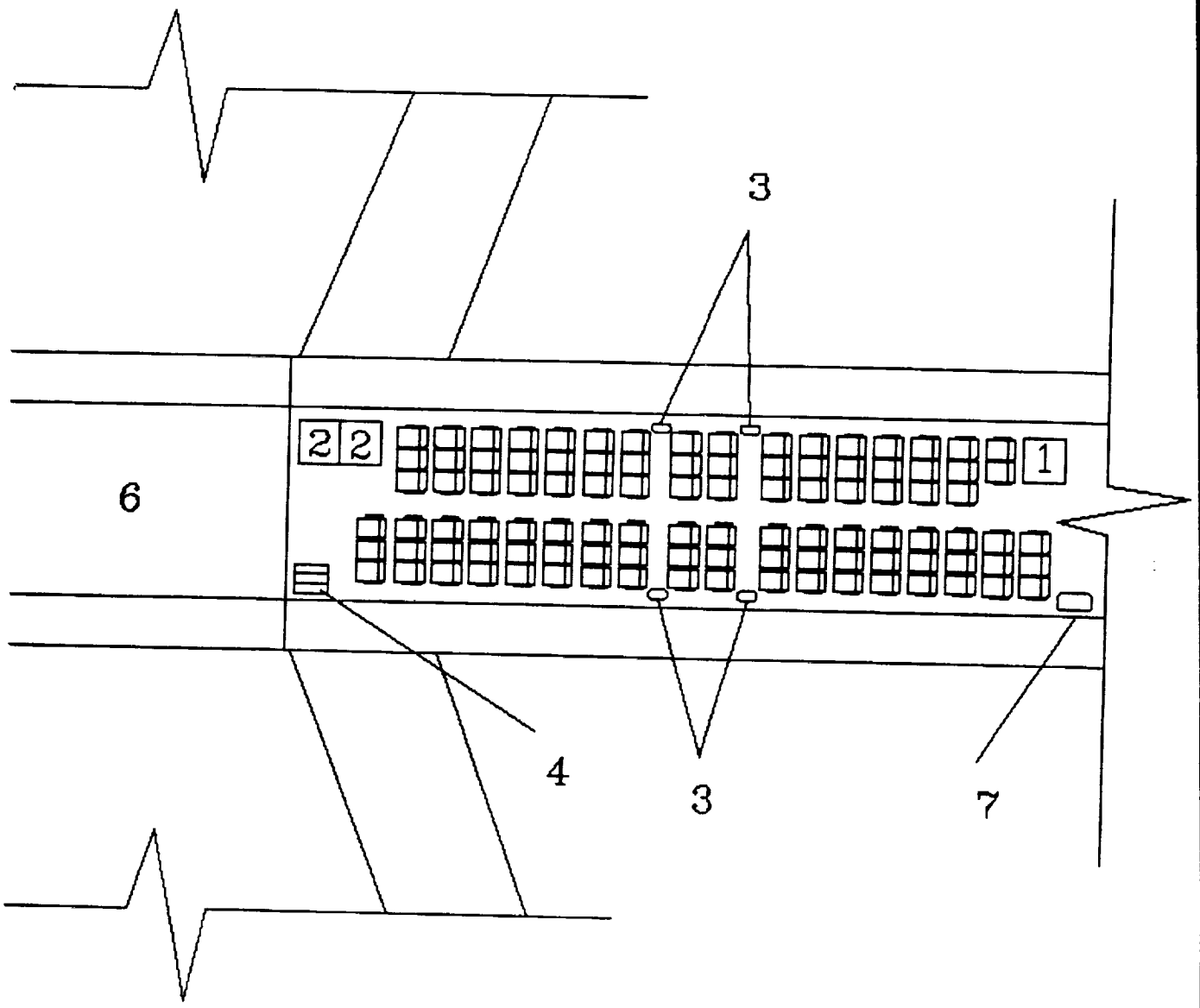

5 – BUNKS
6 – WINGBOX
7 – MAIN EXITS
8 – STORAGE CLOSET

4.3.2.2 Flight Deck The flight deck that was used is similar to the McDonnell Douglas C-17 flight deck because of its high utilization of new technology. The total flight deck crew consists of two 3-member crews consisting of a pilot, copilot, and flight engineer. Due to the extreme length of the design mission (up to 16.5 hours), two flight deck crews will be used to reduce fatigue. A comfortable rest area with three bunks, three seats, a galley, and a storage closet is provided behind the cockpit for the alternate crew.

Pilot workload is reduced with the extensive use of illuminated displays. The cockpit contains a state of the art instrument panel with four multicolor electronic Multifunction Displays (MFDs) and two Head-Up Displays (HUDs). Three of the four MFDs are accessible to each pilot. Each pilot has his own HUD which can be retracted out of sight when not in use. Any available display format can be viewed on any MFD. The display formats which can be selected on the MFDs include:

- Primary flight display formats
- Navigation display formats
- Plan position indicator format
- Engine parameters
- Configuration presentation

Standby electromechanical instruments which display attitude, altitude, airspeed and engine parameters are also provided for each pilot. An automatic flight control system contains controls for flight direction, auto pilot, auto throttle and various navigational functions. All controls which require access from both the pilot and the copilot are centrally located. The aircraft systems are managed from an overhead panel containing the necessary controls and digital readouts (Ref. 12).

4.3.2.3 Cargo Compartment The cargo compartment is sized to hold the volume payload shown in Figure 4.6. The Ostrich, however, is not expected to be able to fly a mission with this payload since the payload's weight exceeds the 800,000 lb. maximum payload set by Reference 1. A sample payload sized to approximately 800,000 lb. is shown in Figure 4.7.

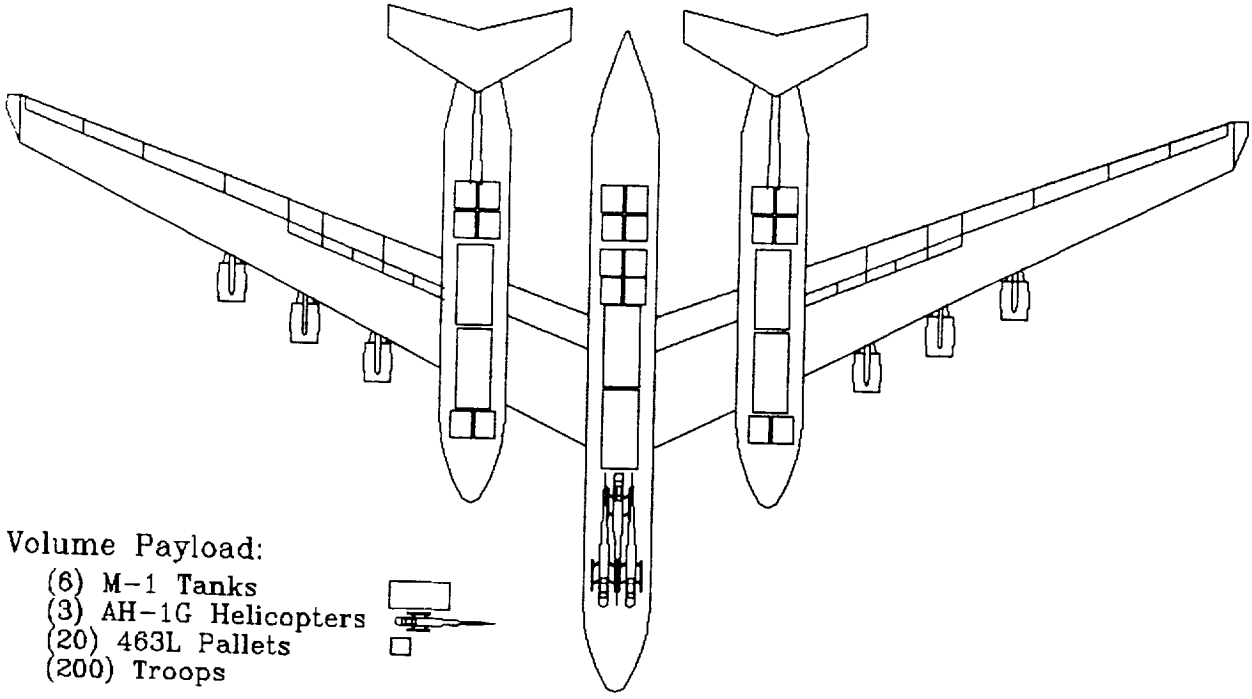

Figure 4.6 Volume Payload Configuration for the Ostrich

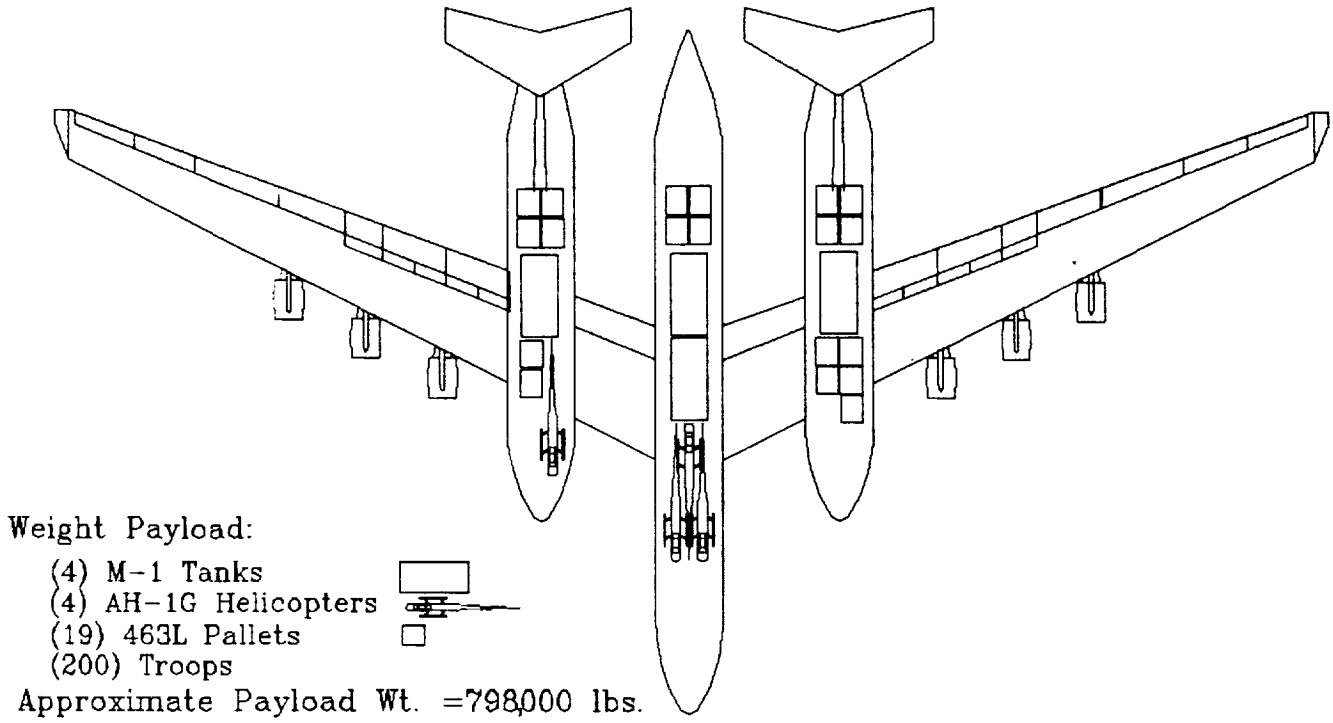

Figure 4.7 Sample Weight Payload Configuration for the Ostrich

The center fuselage cargo bay has an interior height of 13'10" and the outside fuselages have a cargo bay under-wing height of 14'6". This allows for sufficient vertical clearance for the payload specified. Figure 4.8 shows the cargo bay heights of the fuselages.

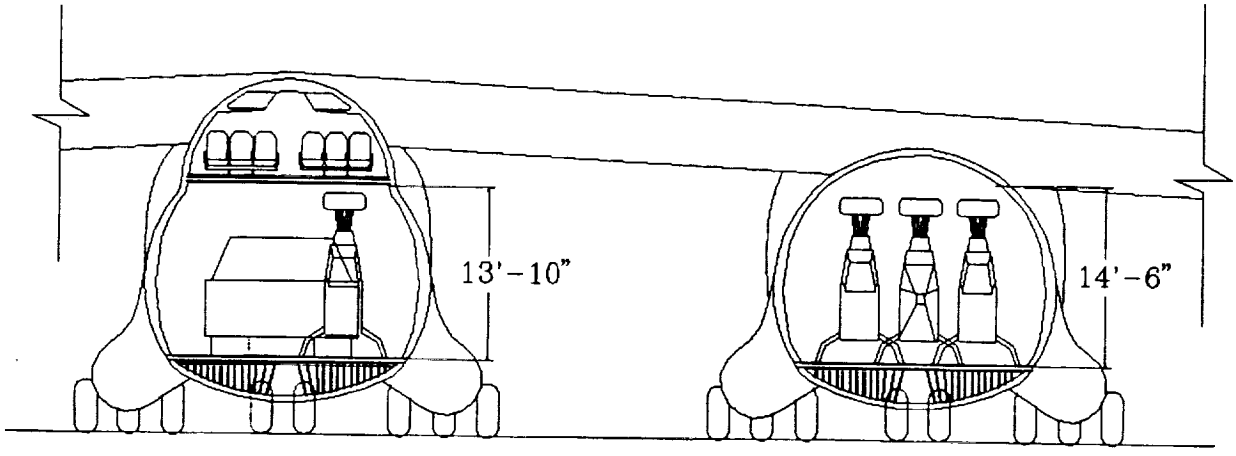

Figure 4.8 Cargo Bay Cross Sections for the Ostrich

A logistics system integrated into the cargo floor of each fuselage, consisting of four rows of conveyers, permits one loadmaster per fuselage operation. The conveyers are easily and quickly inverted to provide a flush cargo floor (Ref. 12).

Each of the three cargo loading ramps are capable of supporting 40,000 lb. in flight and on the ground. To facilitate loading, the ramps drop to an angle of 9 degrees from the static ground line while the cargo doors open inward as shown in Figure 4.9. Four hydraulically powered toes can be positioned vertically during flight or removed and stowed on the upper surface of the cargo door for airdrop missions. The ramp diagram is shown in Figure 4.9.

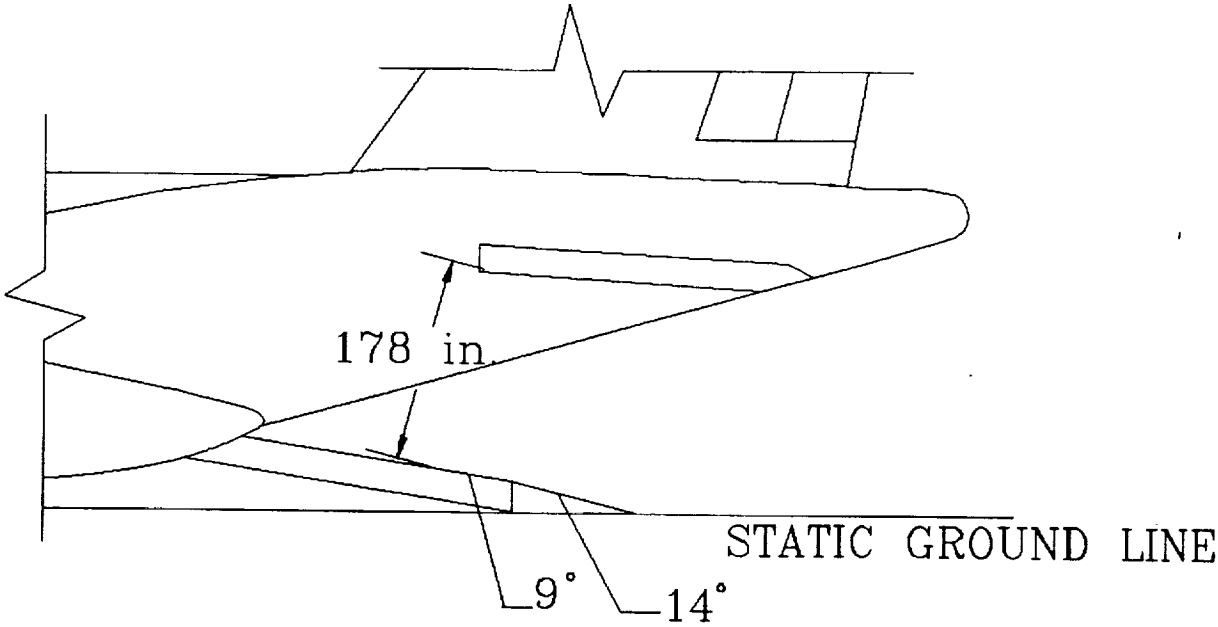

Figure 4.9 Ramp Diagram for the Ostrich

Each cargo compartment has three loadmaster stations from which a single loadmaster can accomplish all of the required duties. The forward station contains aerial lighting controls, delivery controls, cargo door and ramp controls, a communication system, a circuit breaker panel, as well as back up controls for aerial delivery systems and cargo winch. The key features of the left aft control panel include electrical controls, hydraulic controls, cargo compartment loading lights, paratroop airdrop system, APU fire control panel, and manual backup controls for the cargo ramp and door.

4.4 Empennage Design

4.4.1 Configuration Selection

The twin tee-tail configuration was chosen for the Ostrich based upon the comparison of the four tail configurations shown in Figure 4.10. An empennage attached to the center fuselage was not considered because it would interfere with the tails located on the outer fuselages.

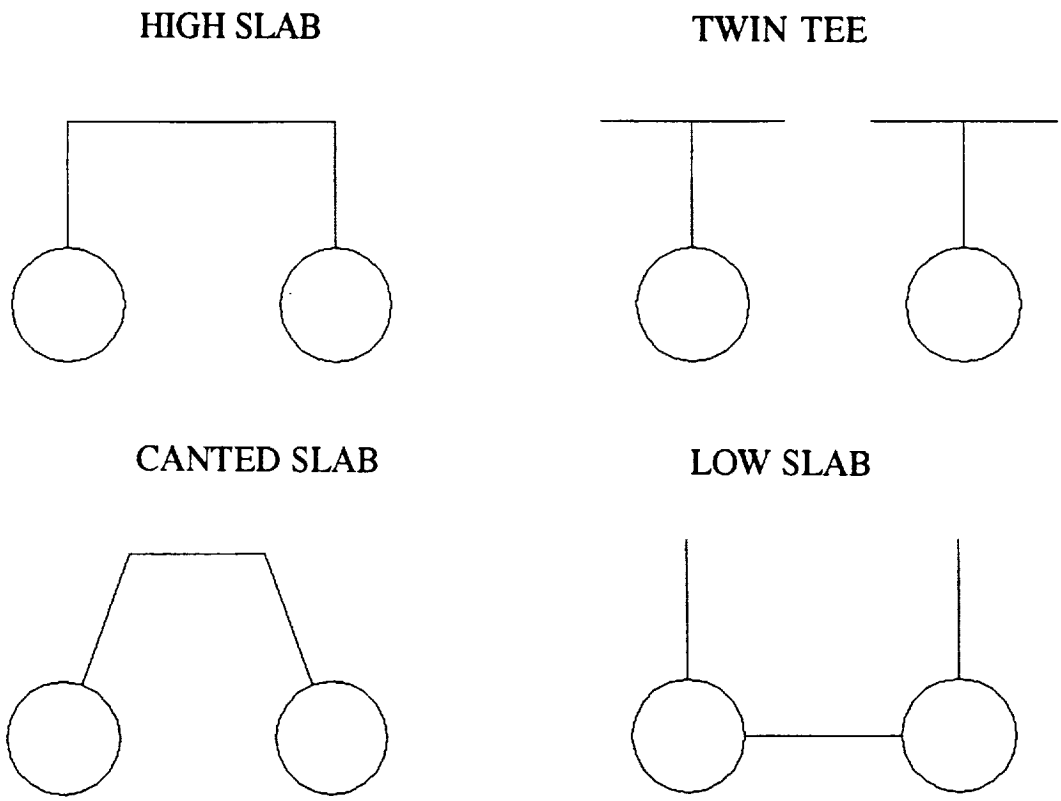

Figure 4.10 Empennage Comparison for the Ostrich

The canted slab configuration did not show any real advantages from a stability and control viewpoint. Control effectiveness is a function of the horizontal and vertical plane projected area. Therefore, for equivalent capability the physical surface area must be larger than the required effective area, and in return has increased weight structurally compared to the other three configurations. Control system complexity is also increased because rudder surface deflections result in a cross coupling force in the longitudinal mode (Ref.20). Additional complexities occur when horizontal and vertical surface controls are deflected simultaneously, causing flow interferences. Unless there were some restriction on the

overall height of the aircraft, there were no foreseeable advantages in using the canted slab.

The high slab tail requires the least horizontal tail area of the four configurations studied, because of the following reasons; it has a longer moment arm, its aspect ratio is higher, and therefore has higher lift coefficients, and the down wash effects from the wing are less. However, due to the moment in the vertical tails, created by the lift in the horizontal tail, and the large span needed to reach across the outside fuselages, the high slab tail will add more structural weight to the aircraft than the twin tee-tail configuration.

The low slab configuration cannot be used on a cargo transport if the aircraft is going to be loaded from the rear of the fuselages, because the horizontal tail interferes with the cargo doors. Also, the down wash from such a large main wing, as the one needed for this size transport, would cause severe down wash problems on the horizontal tail.

To delay drag rise on the horizontal surfaces at the design cruise Mach number of 0.73, two methods were considered. They were sweep, and thickness ratio of the horizontal tails. Because the twin tee-tail was the only configuration which could practically employ sweep on the horizontal surfaces, a thicker airfoil can be used with this configuration, which saves structural weight. The major disadvantage of the twin tee-tail configuration was that it requires larger vertical tail areas than the other configurations due to interference effects from the horizontal tails.

The low slab and canted slab configurations were eliminated for reasons stated earlier. Therefore the two options available for the Ostrich were the high slab and twin tee-tail configurations. The final choice was made based on weight considerations. The additional weight needed for structure considerations in the high slab was found to be more than the

additional weight needed for larger vertical tails in the twin tee-tail configuration. Therefore, the twin tee-tail configuration was chosen for the Ostrich.

4.4.2 Empennage Sizing and Disposition

As a first cut at the initial size and geometry of the horizontal and vertical tails, volume coefficients, aspect ratios, sweep, and taper ratios of other large transports were compared, and then similar characteristics were chosen for the Ostrich. However, a slightly larger vertical tail volume coefficient was chosen to counter critical engine out yawing. Critical engine out yawing would be fairly large on the Ostrich due to engines placed far out the span of the main wing.

The horizontal tail was sized using relaxed static stability criteria and an optimum center of gravity (c.g.) travel. The aft c.g. position is, therefore, limited by stability. The level of relaxed longitudinal static stability selected was initially chosen as an eight percent negative static margin. Static margin will be discussed further in Section 10.0, Stability and Control. This negative eight percent static margin represents the maximum instability that is still controllable (Ref. 14). This insures that the aircraft would remain controllable should a total system failure occur, even at the most adverse c.g. location. The stability augmentation system is designed to provide an equivalent positive five percent static margin to give good flying qualities. The positive five percent static margin is the minimum value stable airplanes are usually designed to(Ref. 20). The most forward c.g. was checked for trim adequacy for the full flap, low speed, landing approach condition. The tail size was also checked for control adequacy during rotation with take-off flaps. The tail selection was made

using the most critical of these three conditions using a maximum lift coefficient of 1.2 which should be easily attainable for the tail.

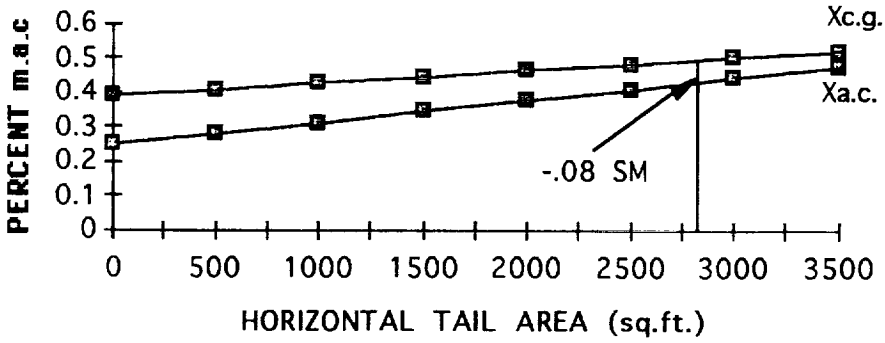

Figure 4.11 Longitudinal X-Plot for the Ostrich

Figure 4.11 is the longitudinal X-plot. It shows the c.g. shift, and aerodynamic center (a.c.) shift as a function of the horizontal tail area. From this plot the tail area which corresponds to a minus eight percent static margin can be read from the horizontal axis. This area is 2600 ft^2. This area was then used to check the two other criteria mentioned in the paragraph above. The tail area was increased to 2900 ft^2 in order to achieve some flexibility in forward c.g. travel for different loading configurations, and still be able to trim at landing. This decreased the static margin to a negative five percent. Trim at landing is the most critical due to the forward c.g. shift from having burned fuel, and the large pitching moment induced by deployed flaps. The trim diagram for landing is shown in Figure 4.12. By increasing the horizontal tail area to 2900 ft^2, the allowable forward c.g. location was increased from .42 to .35

of the mean aerodynamic chord. Other horizontal tail characteristics can be found in Table 4.2.

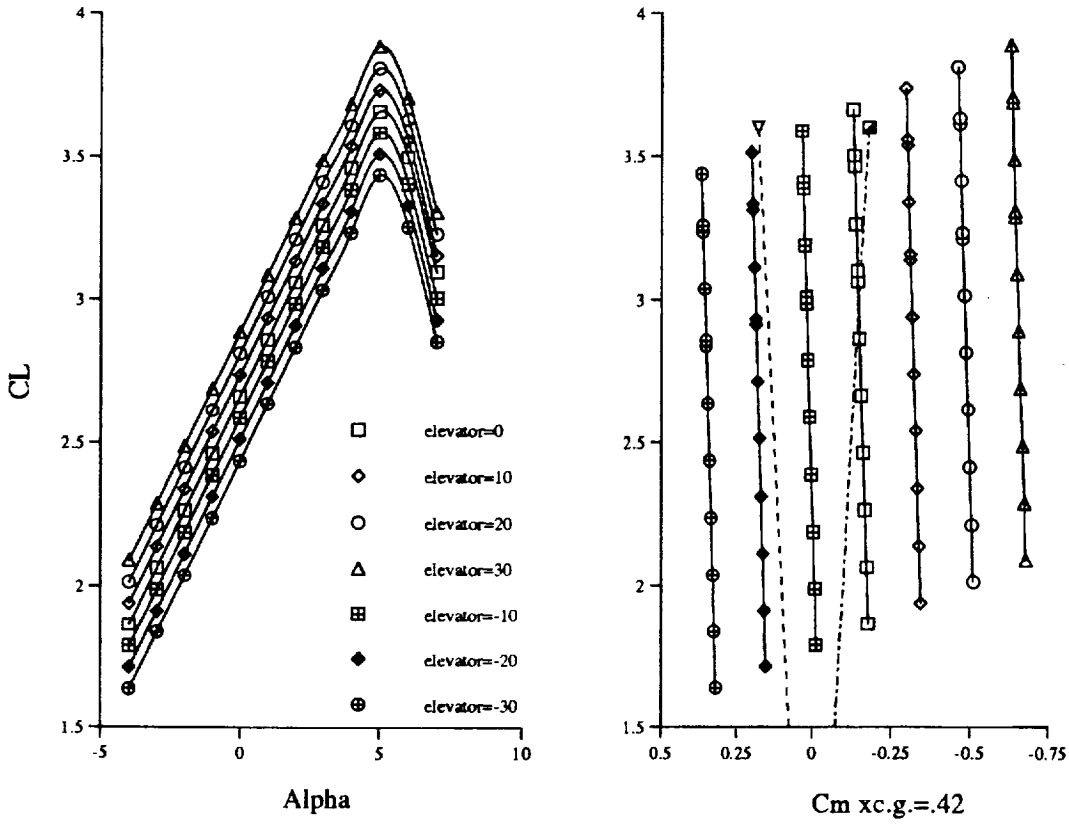

Figure 4.12 Trim Diagram for Landing

The vertical tail was sized for the most critical condition between control of an outboard engine failure on take-off, and minimum level of directional static stability.

For the initial sizing of the vertical tail a directional X-plot was prepared by plotting the yawing due to side slip derivative Cn_β verses vertical tail area. See Figure 4.13. From this plot a vertical tail was chosen to provide a value of Cn_β =0.0015. Based on Lockheed's large transport aircraft experience this value of Cn_β is defined as sufficient to give good flying qualities (Ref. 14). This area is 3,000 ft^2. This area was then used to calculate the rudder deflection needed to overcome a critical engine out during take-off. The rudder deflection was calculated to be 15 degrees with a 30% chord plain flap rudder on 80% of the span. This rudder deflection is an acceptable value (Ref. 20), and therefore the minimal level of directional stability was the critical condition. Other vertical tail characteristics can be found in Table 4.2.

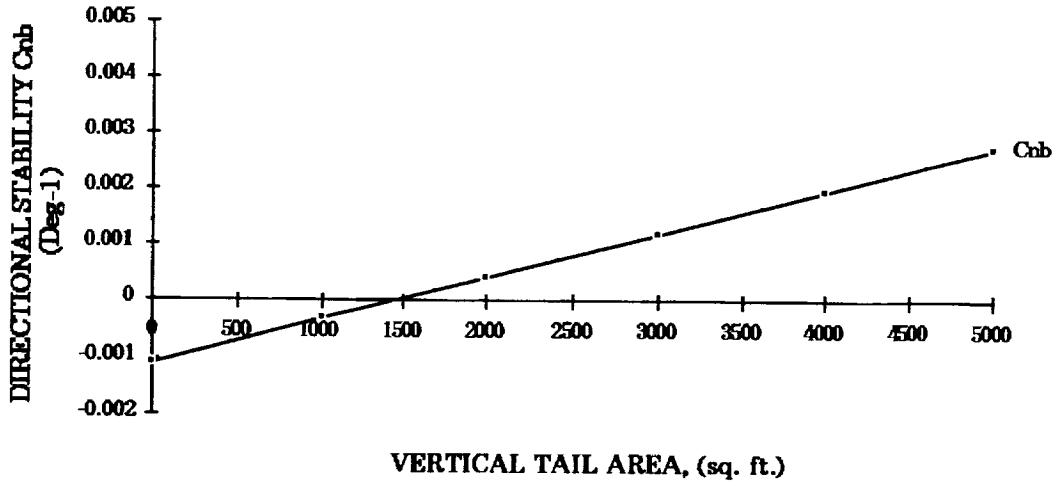

Figure 4.13 Directional X-Plot for the Ostrich

Table 4.2 Empennage Characteristicsfor the Ostrich

Horizontal	**(Single Tail)**
Airfoil	NACA 0012
Area	1,450 ft^2
Span	70.7 ft
Tail Arm	90 ft
Volume Coefficient	.60
t/c	12%
Sweep @ c/4	30°
Vertical	
Airfoil	NACA 0012
Area	1,500 ft^2
Span	47 ft
Tail Arm	80 ft
Volume Coefficient	.048
t/c	12%
Sweep @ c/4	35°

Lateral control is provided by low speed ailerons located on the outer 20% of the wing semispan. Their effectiveness will be discussed in Stability and Control, Section 10.1. There are also high speed flaperons located behind the center engines for lateral control during cruise, because aileron reversal is likely to occur using the outboard ailerons during cruise.

5.0 PROPULSION

5.1 Selection

The amount of thrust needed for the Ostrich was calculated from the design point graph, Figure 3.1. With a thrust-to-weight ratio of 0.24, the required thrust for the Ostrich was 560,000 lbs. It was determined, by the year 2010, engines will be developed that provide a minimum of 90,000 lbs of thrust (Ref. 9), with a SFC of 0.4 required for this aircraft, see Figure 5.1.

The engine chosen for the aircraft is a derivative of the General Electric GE 90, which is currently producing over 100,000 lbs of thrust (Ref. 8). With this thrust, the Ostrich requires six engines.

The GE 90 has a very large fan diameter which increases the bypass ratio to 9. This high bypass ratio will provide a 10% improvement in SFC compared to today's large turbofan engines, while at the same time providing reduced noise levels (Ref. 9). The fan diameter of the GE 90 is 123 inches, with a length of 193 inches.

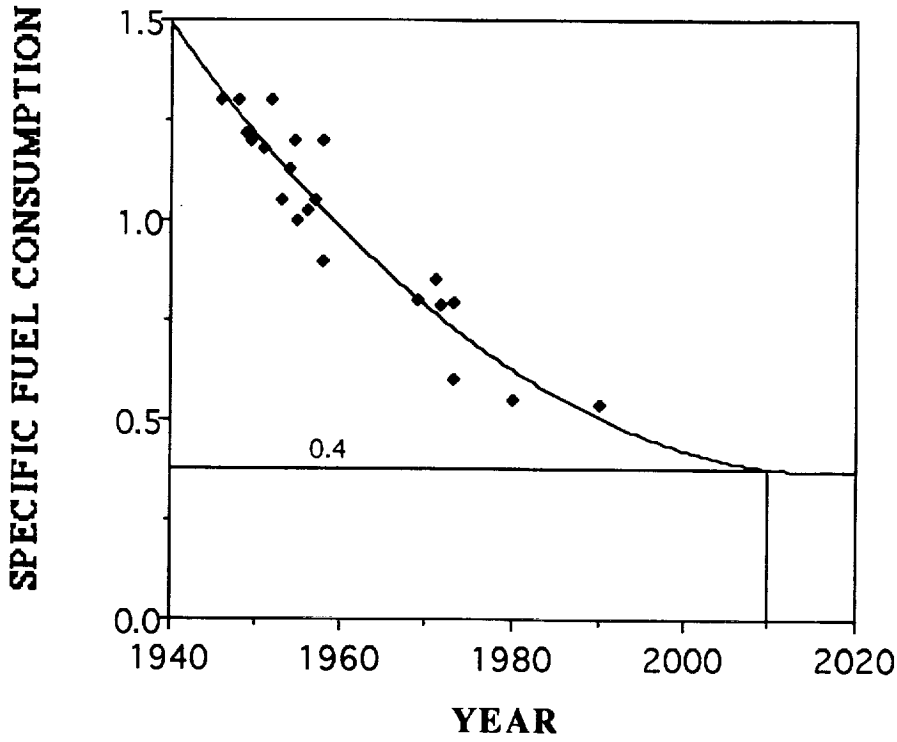

Figure 6.1 SFC vs Time (Ref. 5)

5.2 Engine Placement

The placement of the Ostrich's six engines on the outboard portion of the wing was determined to be the most advantageous position. Other locations considered were the inboard portion of the wing, rear fuselage, and in the vertical tails. Inboard wing mounting of engines was rejected because of the large decrease in lift due to interference effects between the engines and fuselages. Rear fuselage mounting of engines was rejected due to the possibility of down wash from the wing disrupting the airflow into the engines. Tail mounting of engines was rejected due to added structural complexity and reduced engine accessibility. In addition, mounting the

engines on the outboard portion of the wing distributes the weight of the aircraft along the wing more than the other engine placements, thereby further reducing the wing root bending moments which in turn reduces the weight of the wing.

However, there are several problems with this configuration. First, the tail volume must be increased to account for critical engine out moments. Second, there may be a FOD (foreign object damage) problem due to the outboard engines hanging off the edges of the runaway. This is compounded by the anhedral of the wing causing outer engines to sit lower to the ground.

6.0 LANDING GEAR

6.1 Overview

The landing gear for the Ostrich consists of sixteen main bogeys with three wheels each and three nosegear bogeys with two wheels each. The three wheel main bogeys are identical to that used on the McDonnell Douglas C-17 and was chosen for compatibility with the C-17 fuselages. Most of the landing gear components are made from 300M steel which has excellent fatigue strength and fracture toughness compared to other high-strength alloys (Ref 4). The landing gears are electrically controlled and hydraulically operated. In the event of hydraulic failure free fall extension is possible by operating a release lever near each gear which would be operated by the loadmaster stationed in each cargo bay. Shorter fuselages of the three-body design allow for a shorter gear strut to be used for meeting rotation requirements. The landing gear is therefore lighter than it would be on a single fuselage design with the same amount of flotation. This also results in cargo floor heights of about 75 inches, which are also low enough to be compatible with existing ground loading equipment.

A landing gear flotation program obtained from McDonnell Douglas was used to make sure that the Ostrich has sufficient flotation to prevent unacceptable runway damage. Aircraft Classification Numbers (ACNs) were generated for the Ostrich and compared to aircraft already in service. Although ACN is not a method of calculating actual flotations, it is "an excellent method of comparing the flotation of different aircraft" (Ref 4). A low ACN is desirable from a flotation standpoint. The Ostrich has an ACN of 47.3 for a weight of 2,300,000 lbs. on a runway with a California Bearing Ratio (CBR) of 15. The McDonnell Douglas C-17 and the Lockheed C-5A military cargo planes have better flotation, but the Ostrich

still provides a greater amount of flotation than the Boeing 747. This comparison is seen in Figure 6.1.

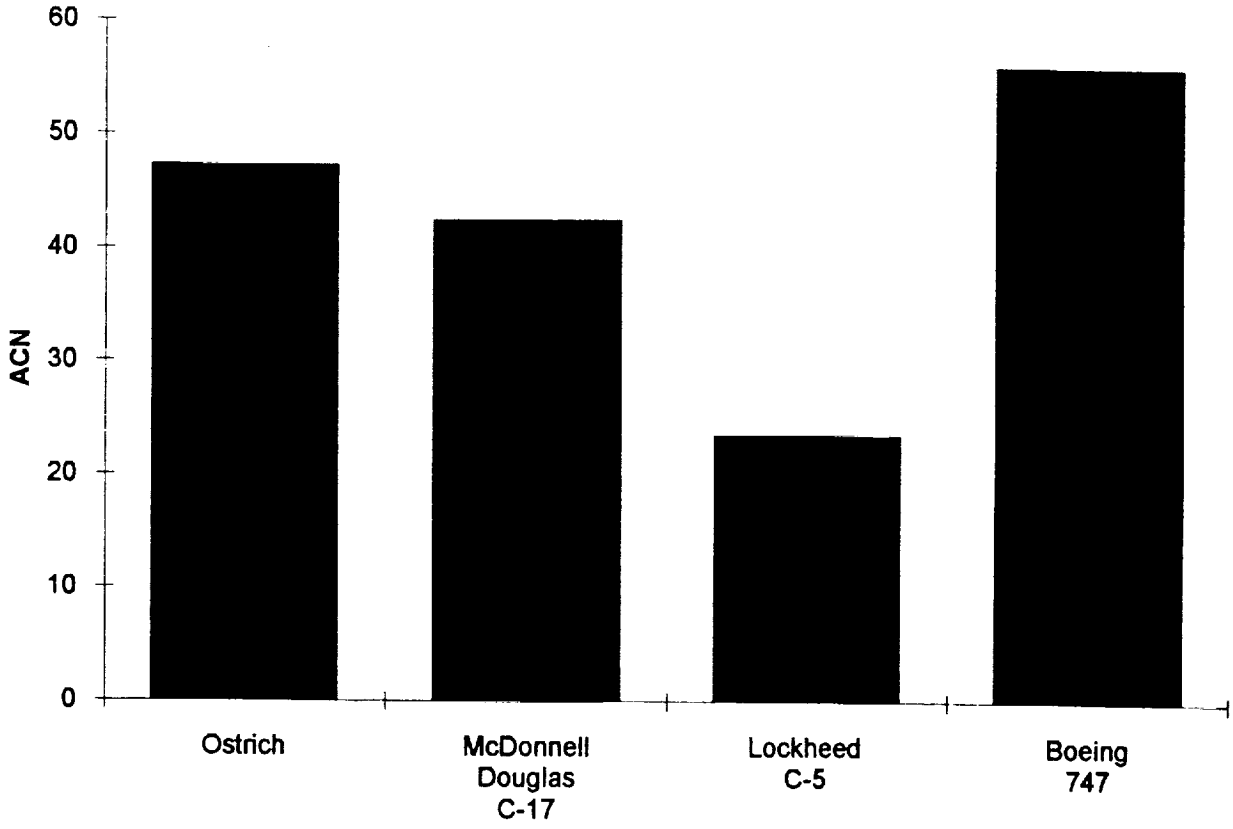

Figure 6.1 ACN Comparison

6.2 Nose Gear

The nose gear for the Ostrich consists of three two wheel bogeys. Each of the nose landing gears retract forward allowing free fall capabilities. The nose gear loadings range from 8% to 11% of the gross take-off weight due to the shift in c.g. This provides sufficient nosewheel traction for adequate steering without exceeding the structural constraints of the nosegear assemblies. Static stability is assured by incorporating positive rake into the nosegear, which tends to lift the aircraft when the nosegear begins to swivel. Dynamic stability is guaranteed by including a

slight positive trail in the nose gear design, causing the runway-to-tire friction to tend to rotate the nosegear back to its original position when it begins to swivel. Positive trail also helps reduce shimmy, an oscillatory dynamic instability. Due to adequate trail and torsion stiffness, a shimmy damper is not needed. A strut travel angle of 7 degrees from its normal position allows the tires to move upwards and backwards when a large bump is encountered (Ref. 4).

6.3 Main Gear

The main landing gear consists of sixteen bogeys of three wheels each. Six bogeys are located on the center fuselage and five bogeys are located on each of the outboard fuselages (three on the outside and two on the inside) as shown in Figure 6.2. Each of the main gears rotate 90 degrees when retracted for a low pod frontal area (Fig. 6.3).

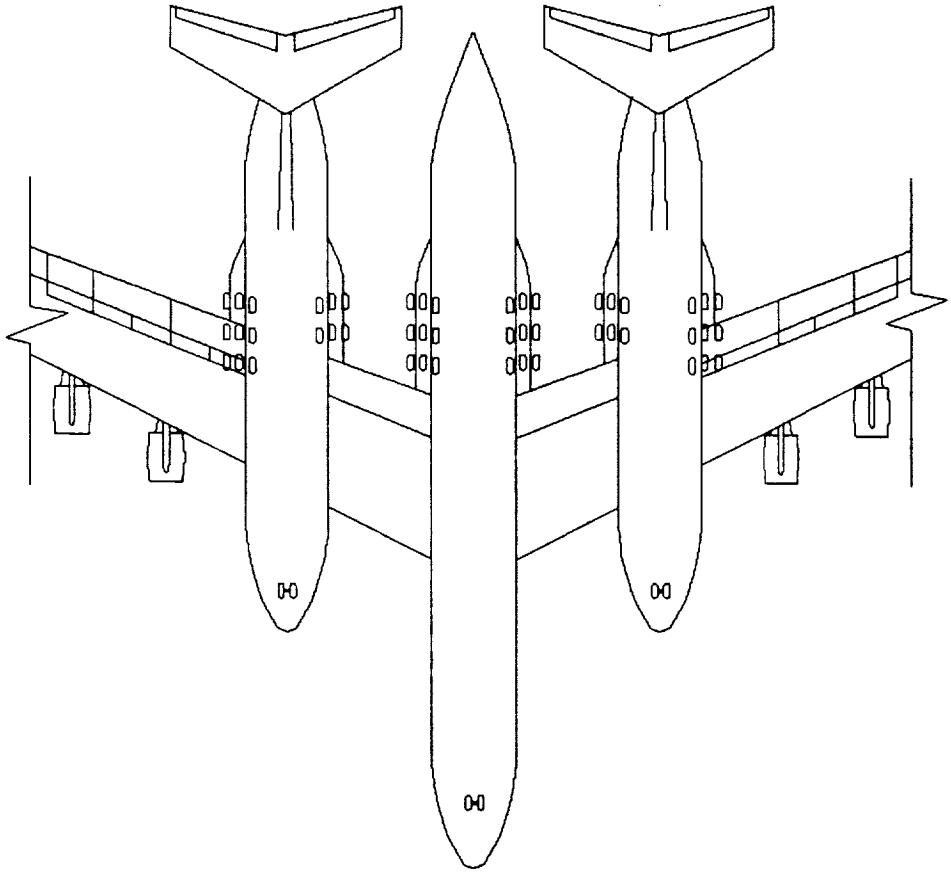

Figure 6.2 Main Gear Placement for the Ostrich

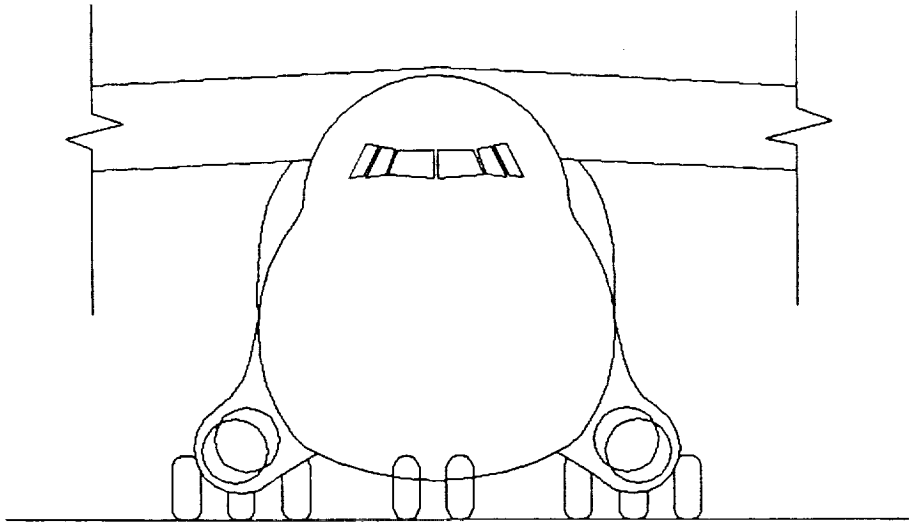

Figure 6.3 Main Gear Retraction for the Ostrich

Conventional air/oil struts are used for shock absorption. The main gear compression stroke needed for a 10 ft./sec. sink rate was calculated to be 15 inches. The main gear shock absorbers have been designed to handle a sink rate of this magnitude without a problem.

The main gear placement allows for a maximum rotation angle of 15 degrees as shown in Figure 6.4. The Ostrich requires a rotation angle of less than 10 degrees at take-off.

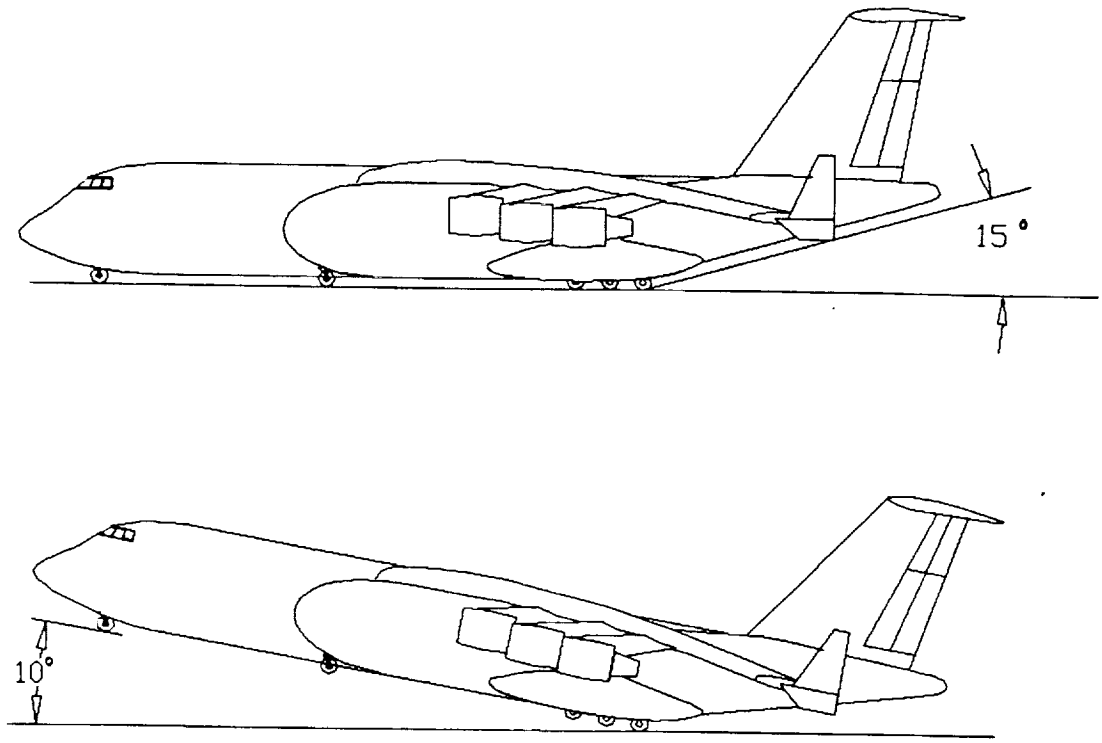

Figure 6.4 Rotation Angle for the Ostrich

The lateral tip over angle, which must not be more than 63 degrees (Ref 22), can sometimes present stability problems, especially for high wing aircraft with high centers of gravity. The Ostrich, because of its wide landing gear placement, has a tip over angle of only 17 degrees as shown in Figure 6.5. Therefore, outrigger gear is not needed on the Ostrich.

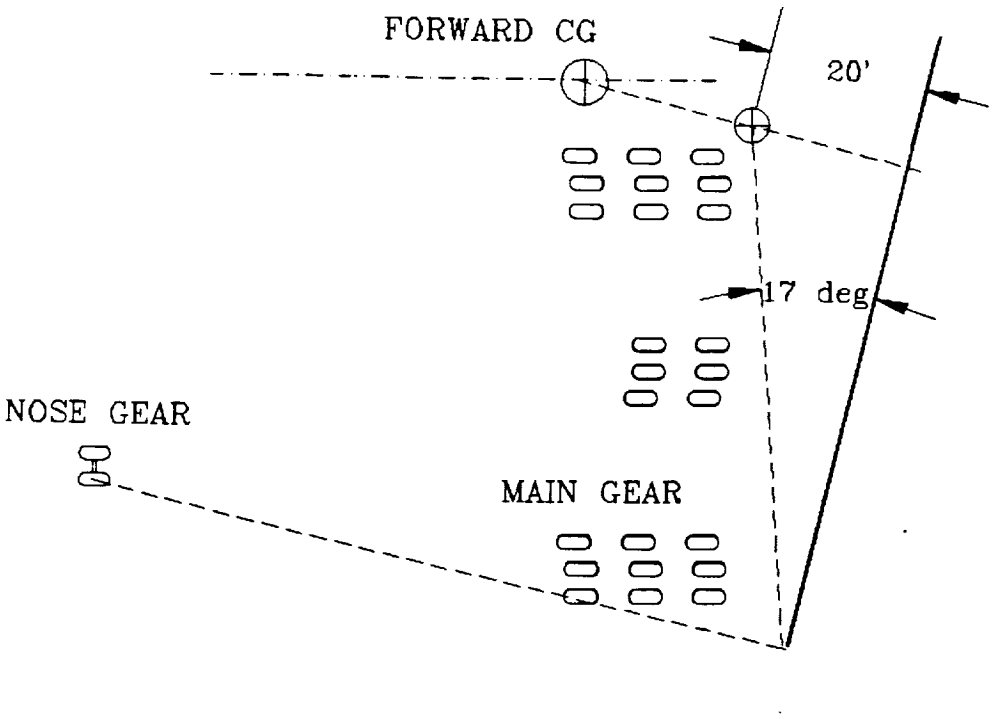

Figure 6.5 Lateral Tip over Layout for the Ostrich

6.4 Brake System

Multiple-disk carbon brakes, which can be controlled symmetrically or differentially, are installed on each of the Ostrich's main gear wheels. Carbon was selected over steel and beryllium for several reasons. The major advantage of carbon heat sinks is weight reduction with equal or superior performance. By switching from beryllium to carbon the Lockheed C-5B was able to save 400 lb per aircraft (Ref 4). High

performance is possible with carbon because of its high thermal conductivity which ensures a more uniform and faster heat transfer rate. In addition carbon retains its strength at high temperatures. Brakes are applied automatically during retraction to prevent wheel rotation. Pressure for emergency braking is provided by accumulators if the hydraulic system failure should occur (Ref. 12).

7.0 STRUCTURES

7.1 Materials

The large size of the Ostrich presented some unique problems for structures. The 2.3 million pound take-off weight required a wing with a very high aspect ratio of 13. By reducing the takeoff weight, the aspect ratio of the wing was reduced. To keep the weight down on the Ostrich, composites were used for much of the structure.

The composite used is graphite/epoxy. This provides high strength and low weight. However, it is brittle and does not yield before failure. The entire structure is 56% composites allowing for a 30% reduction in the empty weight (Ref. 10). The percentage of composites for each component is listed in Table 7.1 and is based on the study of Reference 10. The remaining structure is aluminum. Although today's aircraft incorporate no more than 20% composites in their structures, the trend suggests that by the technology availability date of 2010, most aircraft structures will be primarily composites (Ref. 16).

The wing structure is entirely composites except for the titanium skin on the upper surface and hinges for the control surfaces. The titanium skin is needed for the laminar flow control system. Composites are also used for the empennages, nacelles, pylons, nosecones, and the center fuselage tailcone. This is illustrated in Figure 7.1.

Besides the weight savings, there may be cost savings associated with the use of composites over aluminum (Ref. 10). These include a reduction in operating costs and life cycle costs and will be discussed more in the cost analysis section.

Table 7.1 Weight Reduction Due to Compositesfor the Ostrich

COMPONENT	% COMPOSITES	% REDUCTION
Wing	80	32
Center Fuselage	30	17
Outer Fuselages	0	0
Empennage	85	40
Nacelle & Pylons	80	30
Landing Gear	35	20
Total Structure	56	30
Fuel		16
Take-off Weight		15

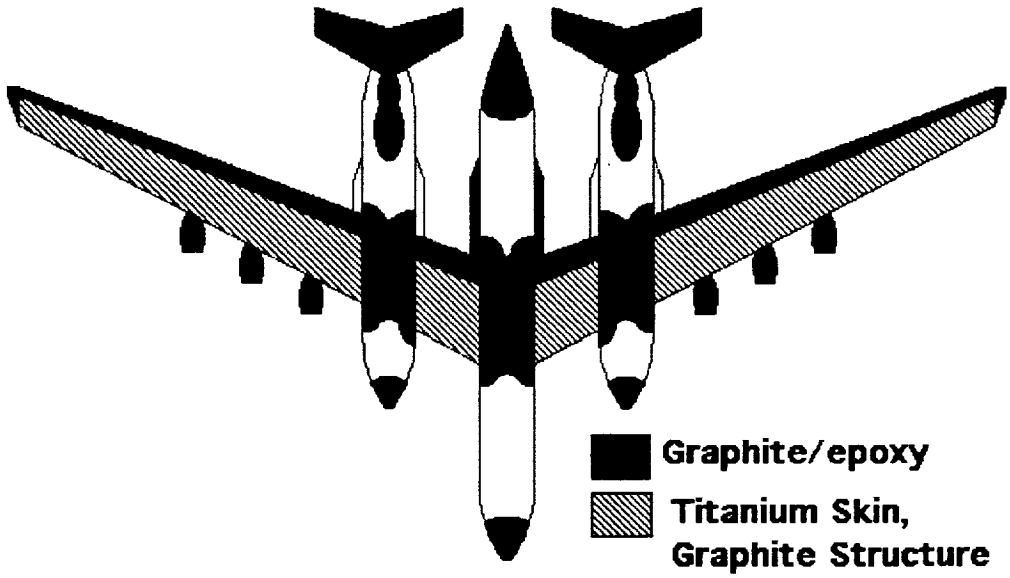

Figure 7.1 Composite Layout for the Ostrich

7.2 V-n Diagram

The V-n diagram in Figure 7.2 was constructed by the method shown in Reference 23. The maximum maneuvering load factors of positive 2.5 g's and negative 1 g's were used as the criteria. The gust critical analysis was done for our cruise speed and altitude of Mach = 0.73 and 35,000 feet, respectively. This set our cruise velocity (V_c) at 292 KEAS. The dive speed (Vd) and maximum structural velocity (V_b) were then found from the graph to be 365 KEAS and 252 KEAS, respectively. Since the gust load criteria from FAR 25 and MilSpecs all fell within the defined maneuver envelope, the aircraft is not gust critical.

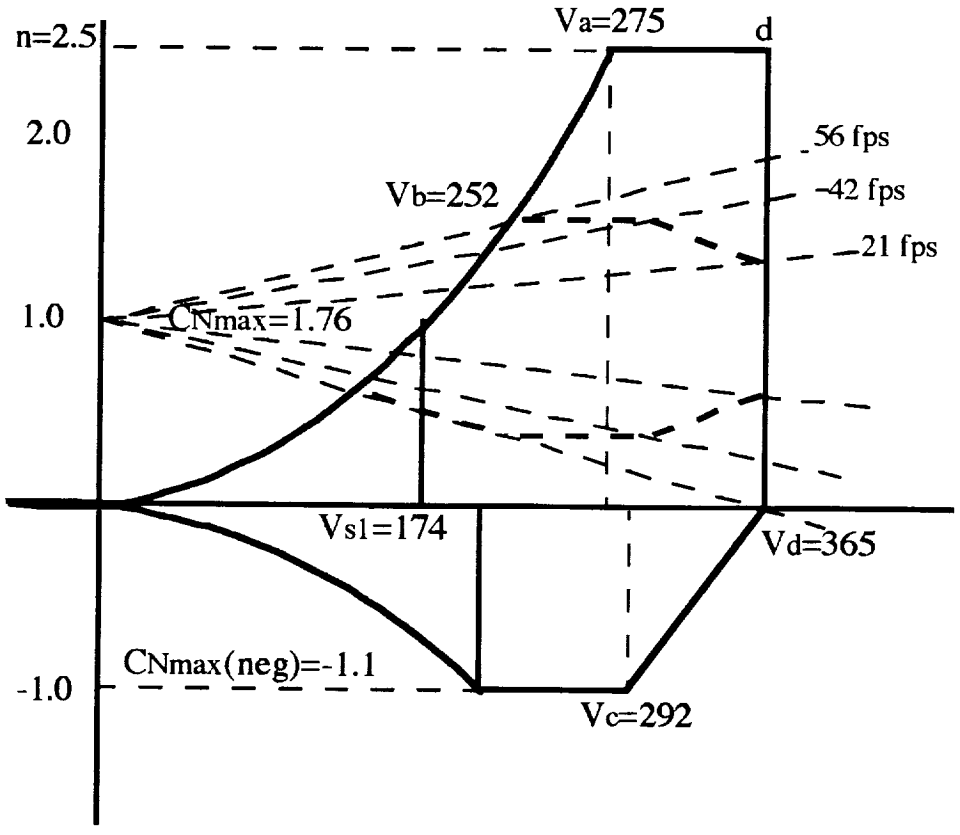

Figure 7.2 V-n Diagram for the Ostrich

7.3 Structural Layout

7.3.1 Fuselages

Conventional methods similar to those used on existing transport aircraft were used to determine the structural layout of the fuselages for the Ostrich. The outside fuselages kept the original McDonnell Douglas C-17 structure except for the empennage and wing attachment points. Due to the larger tail volumes required for this aircraft, the structure had to be reinforced at the tail to accommodate the higher loads.

The main wing placement is different on the Ostrich than it is on the McDonnell Douglas C-17. Therefore, the main ribs on the outside fuselages had to be moved and reinforced to account for the new wing attachment point. Since the outside fuselages no longer needed the flight deck, a composite faring was used to smooth the windshield area.

The center fuselage was designed similar to the Lockheed C-5 fuselage and incorporates much of the same technologies as the McDonnell Douglas C-17 fuselages. By utilizing the McDonnell Douglas C-17 design in the fuselages, considerations in pressure loads due to cabin pressurization and landing gear loads are accounted for.

7.3.2 Empennages

The horizontal and vertical tails followed conventional design characteristics utilizing main spars, stringers, and ribs (Ref. 16). However, with the use of graphite-epoxy composites, the parts can be built stronger and lighter since the fibers can be aligned to create the highest strength in the direction that is most critical (Ref. 7).

7.3.3 Main Wing

The shear and bending moments at the center fuselage were found to be highest when cruising with low fuel. The shear and bending moment for this condition were found to be 474 kips and 24,700 kip-ft., respectively. This is shown in Figure 7.3.

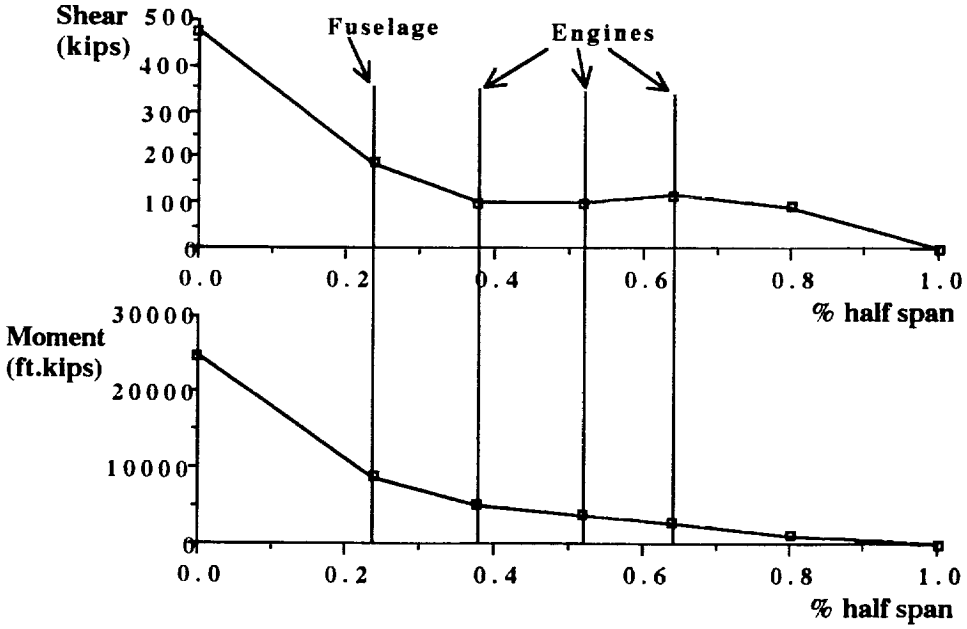

Figure 7.3 Shear and Bending Moment Diagrams for Cruise for The Ostrich

The wing structure was then designed to accommodate these loads and the 2.5g maneuver requirements. The internal structure is shown in Figure 7.4. It incorporates a continuous box that provides the foundation for the outer skin and control surfaces. The combination of the composite 'box' with the titanium and composite skins provides sufficient strength to overcome the shear and bending moments. The continuous center structure provides high strength and torsion resistance and is light weight (Ref. 16).

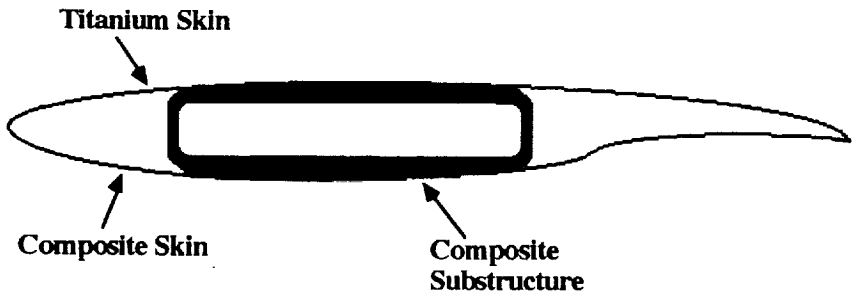

Figure 7.4 Wing Cross-Section for The Ostrich

8.0 AERODYNAMICS

The drag of the Ostrich was determined by using the method found in Ref. 24, chapter 4. The airplane's drag is evaluated by breaking the aircraft into various components that contribute to the drag. The drag calculations of the airplane were evaluated at an altitude of 35,000 ft and a cruise speed of Mach 0.73.

Figure 8.1 gives the drag polars for clean, take-off with landing gear retracted, take-off with landing gear deployed, and landing with landing gear deployed. From the graph, the clean zero lift drag coefficient is approximately 0.022. The take-off zero lift drag coefficient with landing gear retracted is approximately 0.030. The take-off zero lift drag coefficient with landing gear deployed is approximately 0.046, and the landing zero lift drag coefficient is approximately 0.068.

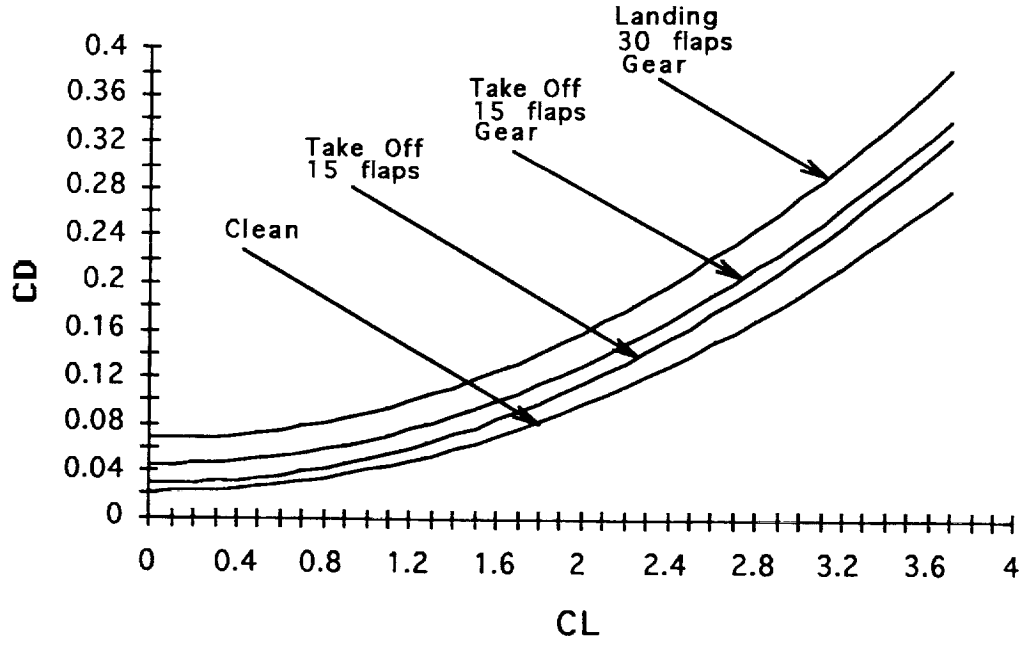

Figure 8.1 Drag Polars for the Ostrich

These drag polars were found using span efficiency factors for clean, take-off and landing of 0.86, 0.80, and 0.75, respectively. These span efficiency factors were determined from Reference 14. A 20% increase in L/D was taken into account due to laminar flow control and future technological advancements such as decreased skin friction drag.

The maximum lift to drag coefficient for cruise in the clean configuration was calculated to be approximately 24. The maximum L/D ratio for take-off with landing gear retracted is approximately 20, and the maximum L/D for landing with landing gear deployed is approximately 12.

A common phenomenon called ground effect occurs when the aircraft is close to the ground. This is the tendency for the aircraft to flare or float above the ground at the point of touch down. This phenomenon becomes more critical as aspect ratio increases and the height of the wing above the ground decreases. The aspect ratio and height of the wing of the Ostrich are 13.3 and 17.5 ft. respectively. Because the Ostrich has such a high aspect ratio these characteristics must be included in the drag polar calculations.

Figure 8.2 compares the drag characteristics in ground effect to that of drag out of ground effect. Figure 8.2 shows that the zero lift drag coefficient is equal in both cases, however, as the lift coefficient increases the drag coefficients diverge. The drag in ground effect significantly decreases as lift increases. At take off with a 15 degree flap deflection, landing gear extended, and a C_L of 2.6, DCD is approximately 0.119 as seen on Figure 8.2. During landing with a 30 degree flap deflection, landing gear extended, and a C_L of 3.2, DCD is approximately 0.242.

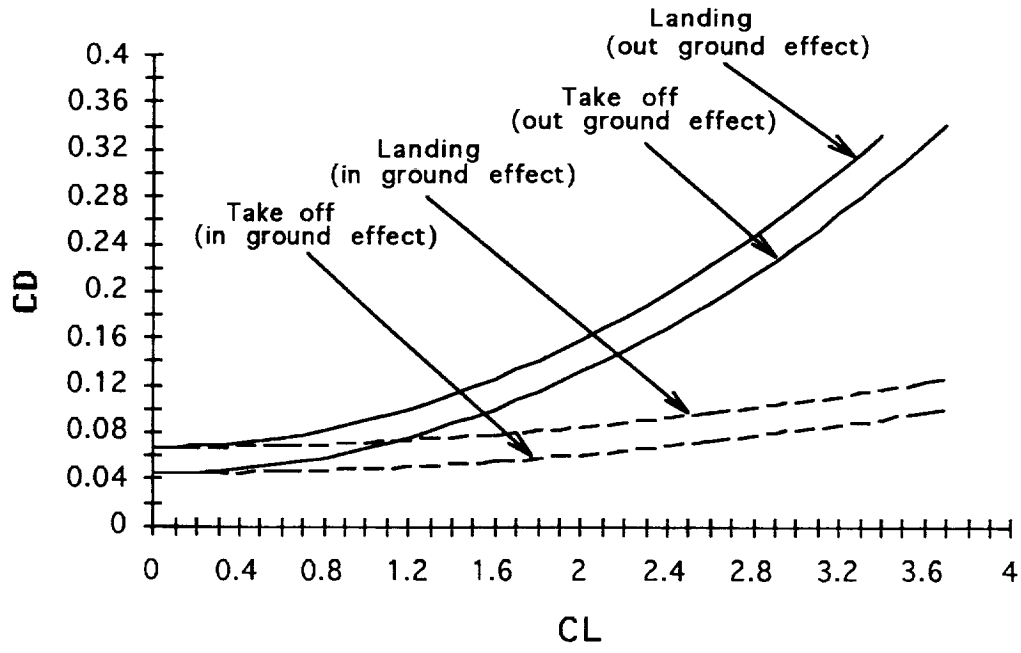

Figure 8.2 In Ground Effect Drag Comparison for the Ostrich

Ground effect needs to be analyzed because it is important in calculating the distance required for take-off and landing. Although ground effect reduces the distance required for take-off, it increases the distance required for landing.

Figure 8.3 shows a total drag break down for the aircraft in trim at cruise. The majority of the drag is produced by the wing. This is due to the contribution of drag due to lift. The drag produced by the wing was reduced by the use of winglets. It can also be seen that the engine nacelles contribute a significant amount of drag to the airplane. This drag includes pylons as well as nacelles. The large drag of the nacelles is due to their large diameter and small fineness ratio. Interference drag is also very significant in the Ostrich because of the three fuselage design.

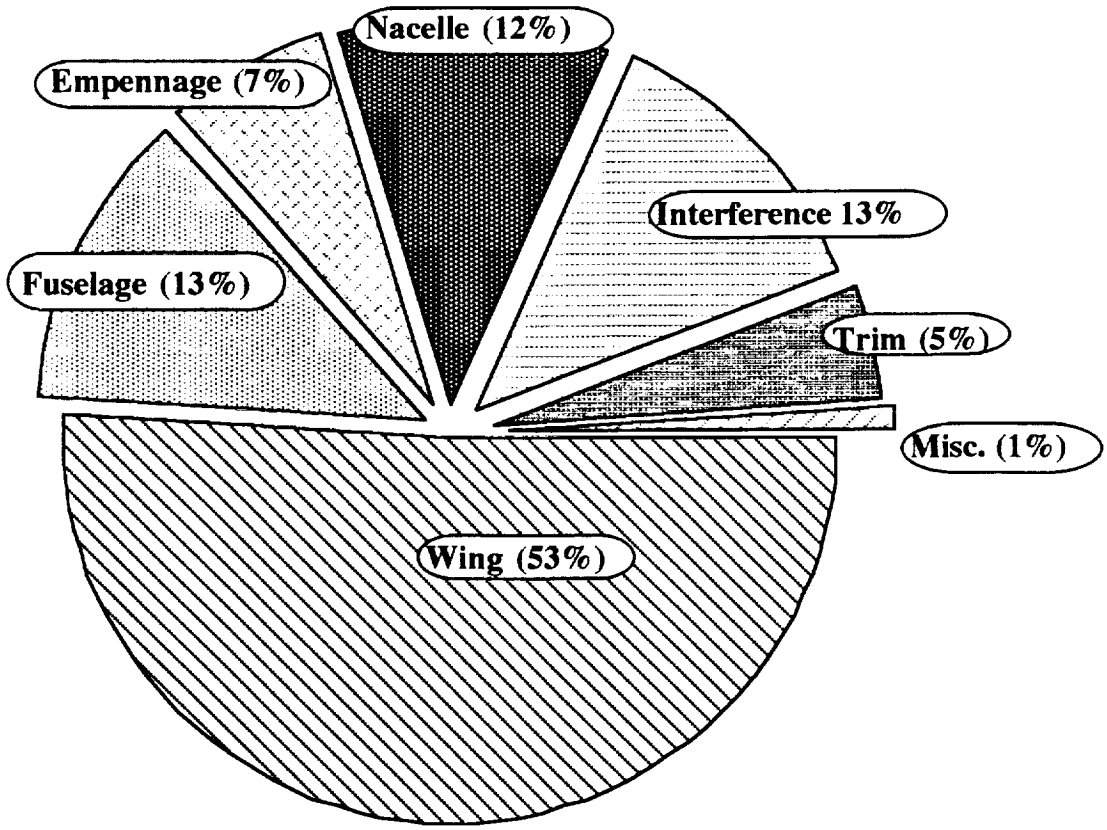

Figure 8.3 Drag Breakdown for the Ostrich

9.0 PERFORMANCE

9.1 Take-Off

The Ostrich was sized to meet the take off and landing requirements stated in Reference 1 and climb gradients specified in Reference 25, appendix B. The regulations require an aircraft to clear a 50 ft. high obstacle at the end of the field on a standard sea level day. The lift off speed (V_{LOF}) is approximately equal to 1.1 times the stall speed at take-off (V_{STO}). The ratio of the speed at the obstacle height to the stall speed is equal 1.15, and the maximum allowable field length is equal to 10,000 ft. Figure 9.1 illustrates these parameters for take off distance.

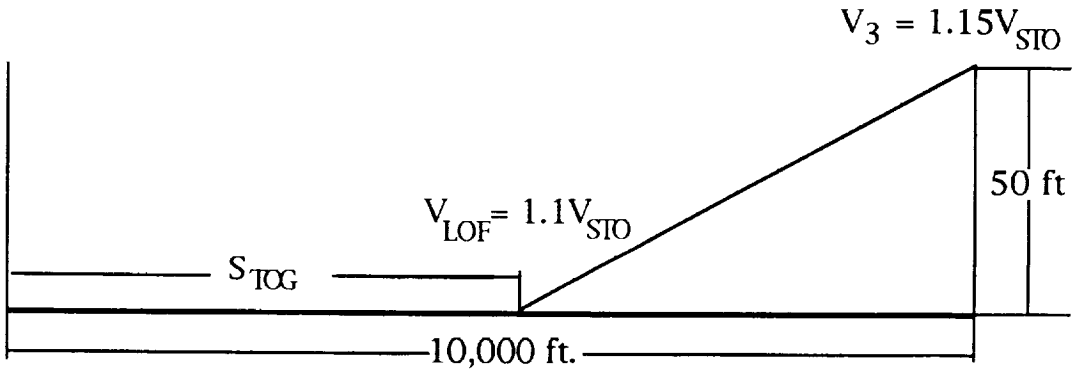

Figure 9.1 Take-off Distance for the Ostrich

The wing loading at take off is 180 psf. The C_{Lmax} at take off is approximately 2.6. The stall speed was calculated to be 139 kts. V_{LOF} is 153 kts, and V_3, the velocity at the obstacle, is 160 kts. Using the method listed in Ref. 25, chapter 5, the take-off distance was calculated to be

approximately 9,867 ft. This value satisfies the maximum field length requirement of 10,000 ft.

9.1.1 Critical field length

The critical field length is defined as the single field length that satisfies the accelerate-stop and take-off requirements. The field length is the distance traveled to accelerate to the critical engine failure speed (V_1) and either continue the take off over a 50 ft. obstacle with one engine inoperative or brake to a full stop. The definition of critical field length is illustrated in Figure 9.2

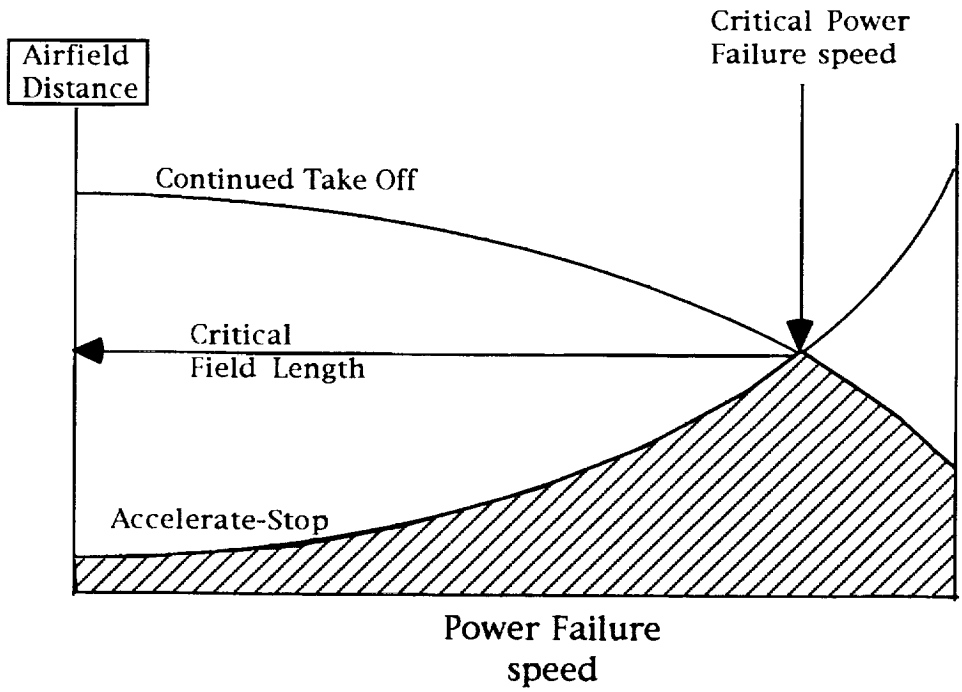

Figure 9.2 Critical Field Length for the Ostrich

The conditions from which the Ostrich can operate safely during a critical power failure are also shown in Figure 9.2. The shaded area of the

graph represents the envelope at which the Ostrich can operate to satisfy the critical field length criteria.

The T/W ratio with one engine inoperative (OEI) is .223, and the L/D ratio with OEI is 11. The L/D ratio with OEI takes into account the increased drag due to wind milling of the inoperative engine and the drag produced by rudder deflection for lateral stability during engine out yawing. The critical field length was calculated to be approximately 8,374 ft., Ref. 25, chapter 5. This satisfies the field length requirement of 10,000 ft. as stated in References 1.

9.2 Landing

Reference 1 requires a maximum field length of 10,000 ft on a standard sea level day for landing. The regulations also require that the airplane clear a 50 ft. obstacle height at the beginning of approach with a minimum approach speed equal to 1.1 times the stall speed (Ref 25). Landing distance is shown in Figure 9.3.

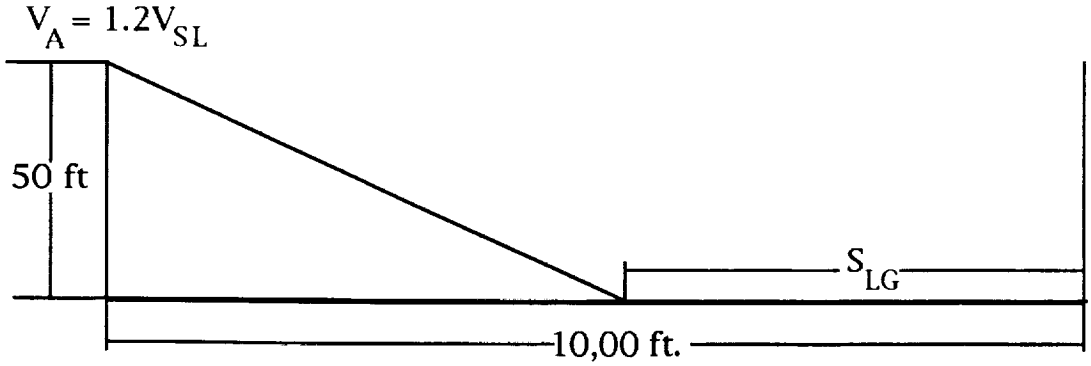

Figure 9.3 Landing Distance for the Ostrich

The stall speed of the Ostrich during landing is approximately 105 kts. The approach speed (V_A) is 126 kts. and the touch down speed (V_{TD}) is 120 kts. The C_{Lmax} at landing is 3.2. The landing ground roll distance (S_{LG}) was calculated to be 1265 ft., and the landing distance (S_L) was calculated to be 2467 ft. A factor of safety of 1.67 was applied to the landing distance to determine the landing field length as stated in the FAR 25 requirements, Reference 25, appendix A. The landing field length was then calculated to be 4112 ft. This meets the requirements of Reference 1, which is 10,000 ft.

The take-off distance, critical field length, and landing distance all meet the 10,000 ft. field length required by Reference 1.

9.3 Climb

The rate of climb (ROC) of the Ostrich can be determined by use of Figs. 9.4 - 9.7. The ROC is evaluated at various altitudes and can be calculated by use of Fig. 9.4 - 9.6. These figures are the power curves for the Ostrich at sea level, 30,000 ft., and 35,000 ft. respectively. These curves were calculated through methods found in Reference 2, chapter 6.

The maximum ROC at each respective altitude can be determined by calculating the maximum excess power ($P_{available}$-$P_{required}$), and dividing this difference by the take-off weight of the aircraft, provided that the climb angle g is less than 20°. The climb angle g is the angle between the horizon and the flight path of the aircraft. It was found that g is typically less than 15° in all aircraft except for fighters (Ref. 2). Figures 9.4 - 9.6 show that the values for excess power are of 144 million, 28.8 million, and 4.6 million ft-lb/s respectively. The take-off weight of the

Ostrich is 2.3 million pounds. Therefore, the initial ROC's are 3,757 fpm, 751 fpm and 120 fpm for altitudes of sea level, 30,000 ft. and 35,000 ft.

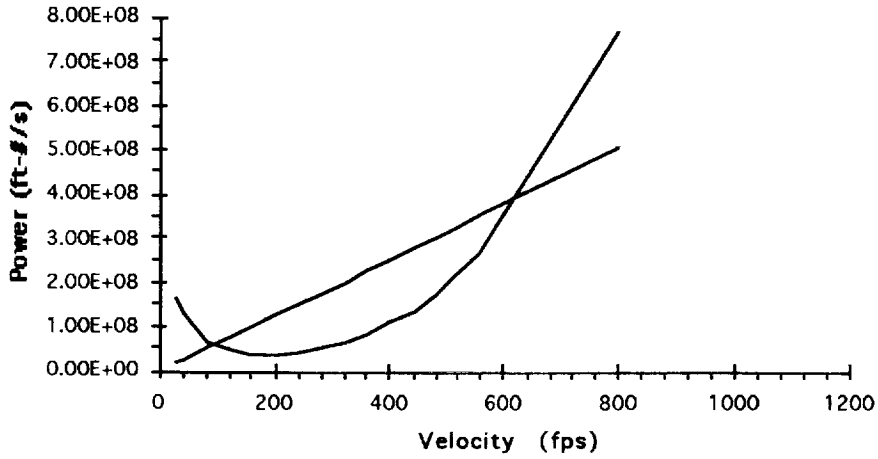

Figure 9.4. Variation of Excess Power at Sea Level for the Ostrich

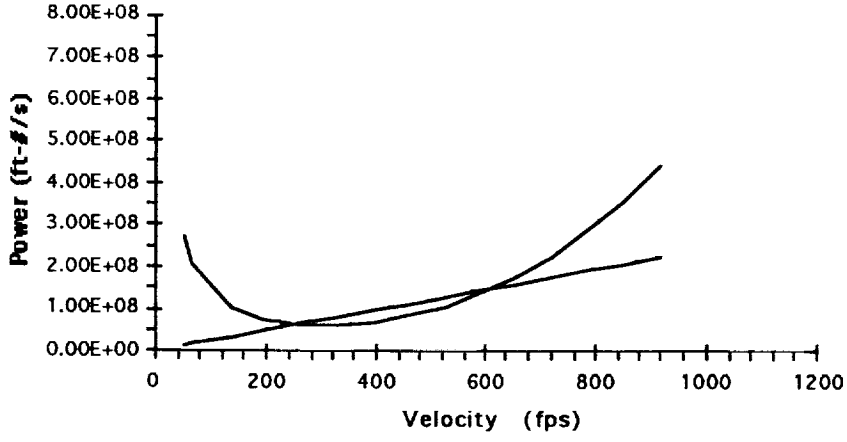

Figure 9.5. Variation of Excess Power at 30,000 ft. Altitude for the Ostrich

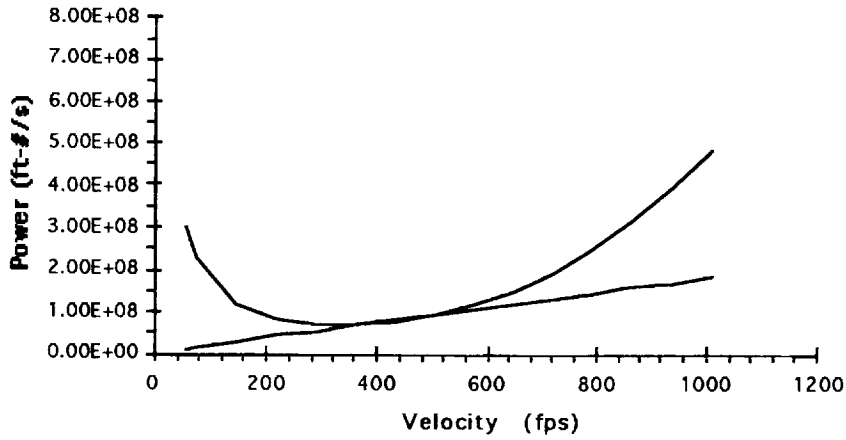

Figure 9.6 Variation of Excess Power at 35,000 ft. Altitude for the Ostrich

Rate of climb is an important design consideration because of the need to know the aircraft's capabilities during adverse conditions. The aircraft must be able to adequately climb to higher altitudes in order to avoid weather or to minimize air traffic problems. Weather conditions are especially important for the Ostrich because of the wing's tendency to twist due to the outer fuselages.

9.4 Absolute and Service Ceiling

The absolute ceiling of an aircraft is defined as the altitude at which the ROC is equal to zero. The absolute ceiling can be found by plotting the variation of ROC with altitude. Fig. 9.7 is an example of this plot for the Ostrich. The ROC values used were previously calculated in Section 9.3.

The relationship between altitude and ROC is very close to linear. Therefore, it is safe to assume a linear relationship and plot a straight line

approximation through the data. Fig. 9.7. shows that the ROC linearly decreases as altitude increases. From this plot an absolute ceiling of approximately 37,000 ft. is estimated. A more practical quantity that is used is called the service ceiling. The service ceiling is the altitude at which the maximum ROC is equal to 100 fpm. From Fig. 9.7, the service ceiling is approximately 36,000 ft.

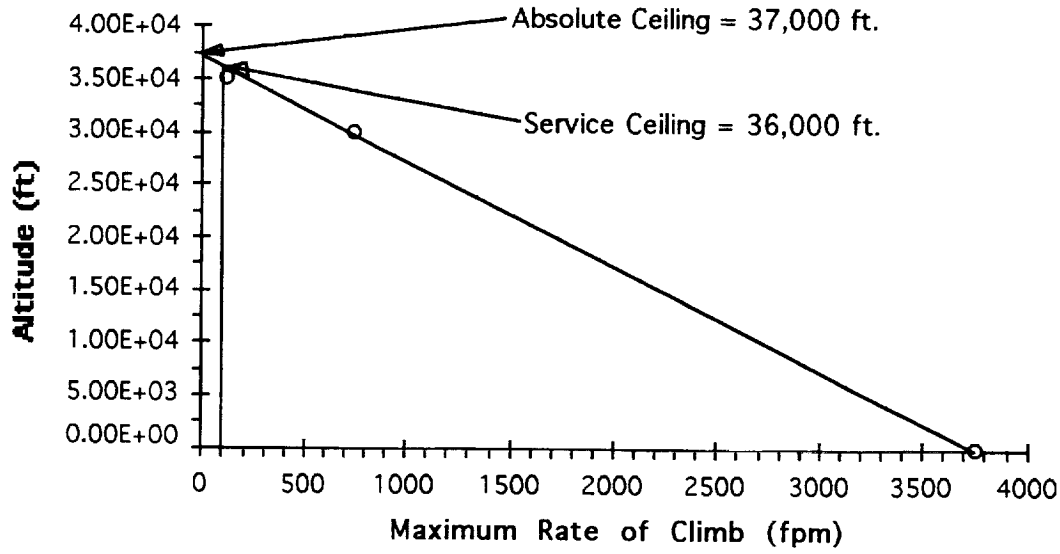

Figure 9.7 Absolute and Service Ceiling for the Ostrich

The absolute and service ceiling give the envelope at which the Ostrich can operate. Therefore the Ostrich is limited to flying at altitudes lower than the service ceiling of 36,000 ft. The Ostrich is flying at an optimum cruise altitude of 35,000 ft. Therefore the Ostrich meets the ceiling requirements calculated in this section.

9.5 Payload Range Diagram

There are four critical points in the payload range diagram, Figure 9.8. At point 1, the Ostrich has a range of zero with a full payload weight of 800,000 lbs. and no fuel on board. At point 2, the diagram shows a range of 13,000 nautical miles. This point is sometimes called the harmonic range and is defined as the point at which the aircraft is at full payload and full fuel without exceeding maximum take-off weight. Between points 2 and 3, payload weight is traded for fuel weight until the aircraft reaches it's volumetric fuel capacity. This allows the Ostrich to have a maximum range of approximately 22,000 nautical miles at maximum take-off weight. At point 4, the Ostrich is at ferry range of 28,000 nautical miles with zero payload and full fuel.

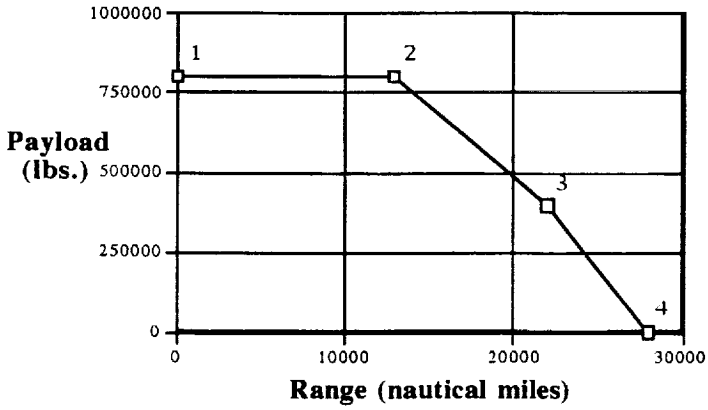

Figure 9.8 Payload vs. Range for the Ostrich

10.0 STABILITY AND CONTROL

10.1 Weight and Balance

Most of the component weights for this aircraft were estimated using the empirical relations presented in Reference 23. However, the weight of the engines was estimated from data supplied by General Electric.

The fuel was situated as close to the c.g. as possible to limit the c.g. travel during a mission when the fuel is burned. The wing was moved forward from the original configuration so that the c.g. is located forward from the main landing gear in order to meet the longitudinal tip-over criteria. The location of the landing gear meets the lateral and longitudinal criteria. A c.g. diagram is shown in Figure 10.1. The fuselage station is measured from the nose of the aircraft. The c.g travel for this mission is 3.3 feet or 10% of the mean aerodynamic chord, which corresponds to .42 and .52 percent of the mean aerodynamic chord. As mentioned earlier the horizontal tails were sized to allow a maximum forward c.g. travel to .35 percent of the mean aerodynamic chord to allow some flexibility for different loading configurations.

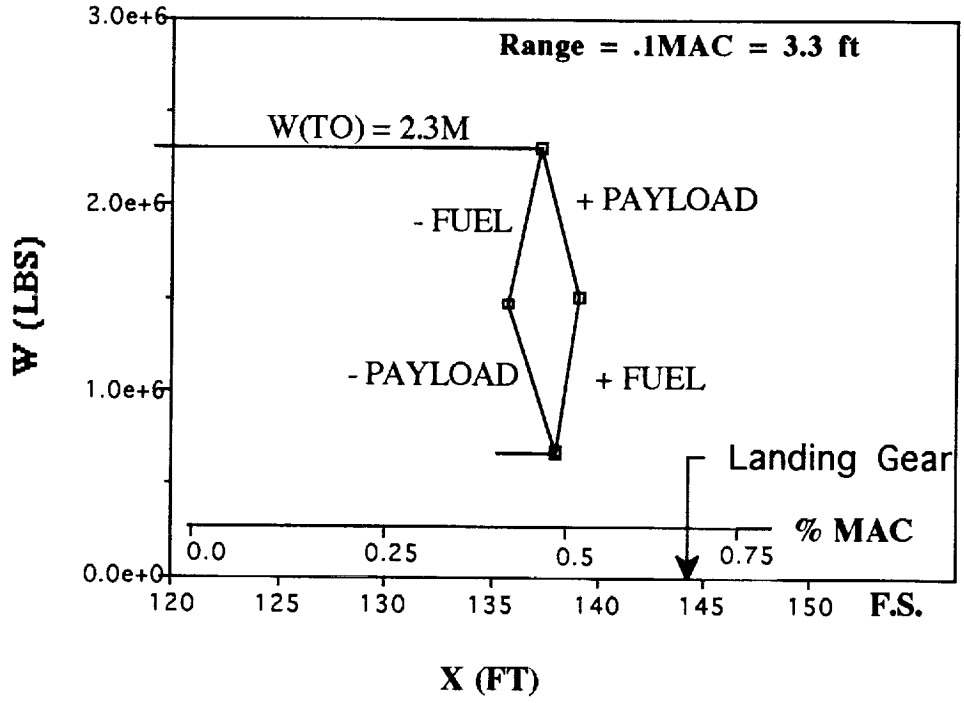

Figure 10.1 C.G. Excursion for the Ostrich

10.2 Stability Derivatives

The stability and control derivatives were estimated using the equations and graphs presented in Reference 24 and Reference 6. Because of the multibody configuration, simplifying assumptions had to be made and simple equations had to be derived for the effect of body and tail offset on the derivative components. Further study is necessary to more exactly define these effects. Two flight conditions were chosen to represent the cases of most interest in the operational flight envelope of the Ostrich. These conditions are landing approach, $1.3V_S$ at sea level, and cruise M=.73 at 35,000 ft. The stability level shown for all aircraft represents an effective positive five percent static margin, dC_m/dC_L=-.05. The stability derivatives for the Ostrich are listed in Table 10.1.

Table 10.1 Stability Derivatives

UNITS: 1/RAD	LANDING CASE	CRUISE CASE
C_{L_α}	9.68	9.68
C_{M_α}	-.289	0.289
C_{M_α}	-9.46	-13.4
C_{M_q}	-4.58	-10.5
$C_{M_{\delta e}}$	-1.23	-1.07
$C_{L_{\delta e}}$	0.38	0.32
$C_{M_{i_H}}$	-2.91	-3.21
$C_{L_{i_H}}$	0.79	0.84
C_{n_β}	.14	0.149
C_{l_β}	-.12	-0.019
C_{y_β}	-.86	-0.79
C_{n_p}	-.092	-0.048
C_{l_p}	-.41	-0.62
C_{y_p}	-.198	-0.29
C_{n_r}	-.175	-0.181
C_{l_r}	.18	0.19
C_{y_r}	0	0
$C_{n_{\delta r}}$	-.0723	-0.063
$C_{l_{\delta r}}$	.0169	0.0092
$C_{y_{\delta r}}$	.29	0.17
$C_{n_{\delta a}}$	-.0024	-
$C_{l_{\delta a}}$	-.105	-

10.3 Static Stability

The longitudinal static stability parameters were initially calculated in the empennage sizing and design, Section 4.4. Longitudinal static stability as discussed here refers to dC_m/dC_L, the change in pitching moment with the change in lift.

Static margin is defined as the distance from the total aircraft center of gravity (c.g.) to the total aerodynamic center (a.c.) in percent of the mean aerodynamic chord. The static margin is defined as positive if the center of gravity is forward of the a.c. A positive effective static margin is necessary for a statically stable aircraft. Conventional aircraft designs usually have a minimum positive five percent static margin (i.e. dCm/dCL = -0.05) Reference 20.

However, the Ostrich incorporates the concept of reduced longitudinal static stability to decrease horizontal tail size. Assuming a five percent static margin as the base, going to the condition of minus five percent reduces the horizontal tail area by 20 percent. This instability is offset with a fly-by-wire augmentation system, increasing the effective stability to give good flying qualities. The fly by wire system will also cut down on the pilots work load during heavy task maneuvers such as, air drops. Fighter aircraft have been using reduced longitudinal static stability for many years, and now even some transports, such as the Airbus 320 and the McDonnell Douglas C-17, are using the fly-by-wire augmentation system. Therefore, by the technology availability date of 2010 given in Reference 1, many planes will have relaxed longitudinal stability. As expressed in the empennage sizing and design, Section 4.4, the horizontal tail is sized for a negative five percent static margin, which represents an instability that is still controllable in case of an all out failure of the

augmentation system. And with the augmentation system operational the effective stability is at least five percent.

Directional static stability is also initially defined in the empennage sizing section. The tail sizing calculations size the vertical tail for engine out trim and minimum directional stability. From other large transport data such as the Lockheed C-5 and McDonnell Douglas C-17, it was found that a minimum C_{n_b} of .0015 per degree. is defined as sufficient to give good flying qualities (Ref. 20). For the Ostrich the minimum directional stability is the critical sizing criteria, and therefore the vertical tails were sized to this requirement.

10.4 Dynamic Stability

The dynamic modal parameters and aircraft response to control inputs are computed using the equations presented in Reference 25.

Table 10.2 presents the dynamic stability modal parameters for the Ostrich. The longitudinal parameters are computed for an effective five percent static margin, which is the normal augmentation operative case. This represents the level of stability that the fly by wire augmentation system will provide.

Table 10.2 Modal Parameters for the Ostrich

LONGITUDINAL	LANDING	CRUISE
PHUGOID (5% EFFECTIVE SM)		
Damping Ratio	.356	.049
Natural Frequency (rad/sec)	.115	.0435
Period (sec)	54.6	144.4
SHORT PERIOD (5% EFFECTIVE SM)		
Damping Ratio	.980	.896
Natural Frequency (rad/sec)	.498	.782
LATERAL		
SPIRAL MODE		
Time to Double (sec)	54.7	68.2
DUTCH ROLL		
Damping ratio	.148	.132
Natural Frequency (rad/sec)	.362	.569
Frequency-Damping Product	.054	.075
Period (sec)	42.5	47.6
ROLL MODE		
Time Constant (sec)	1.39	1.19

Performance is considered adequate if the augmented aircraft meets level 1 flying qualities, which are defined as clearly adequate for the mission flight phase. Level 2 is defined as adequate flying qualities but with an increased pilot workload or degradation of mission effectiveness. Level 3 is defined as flying qualities such that the aircraft is controllable but the pilot workload is excessive or the mission effectiveness is inadequate (Ref.25).

The Level 1 requirement on the phugoid damping ratio is that it be equal to or greater than .04 (Ref.25). The Level 1 requirement on short period damping is $.35<z_{sp}<1.3$ for category C, and $.3<z_{sp}<2.0$ for category B (Ref.25). The Ostrich meets these requirements. The short period frequency of the Ostrich is too low to meet Level 1 requirements,

however the Lockheed C-5 also has short period frequencies below the requirements, but its flying qualities are rated good (Ref.14).

The Dutch roll mode requirements call for a minimum damping ratio of .08 for Level 1 and .02 for Level 2 (Ref.25). The minimum frequency requirement is given as .4 rad/sec (Ref.25). A combination requirement is given also as a minimum frequency damping ratio product of .15 for level 1 and .05 for level 2 (Ref.25). The Ostrich does not meet the natural frequency requirement on landing, and the frequency damping product only satisfies Level 2 requirements. However conventional augmentation systems should provide good flying qualities.

The roll mode time constant requirement is for a value no greater them 1.4 for Level 1 (Ref.25). The Ostrich meets this requirement both in cruise and landing.

Spiral stability is stipulated by requiring the time to double amplitude be at least 20 seconds for Level 1 (Ref.25). Again the Ostrich meets this requirement, and may be too stable.

10.5 Control Power

One example of control requirements is the ability to land in a crosswind. The required rudder and aileron deflections to land in a 90 degree crosswind are presented in Figure 10.2. The Ostrich is able to achieve a zero crab angle touchdown in a 35 kt. crosswind.

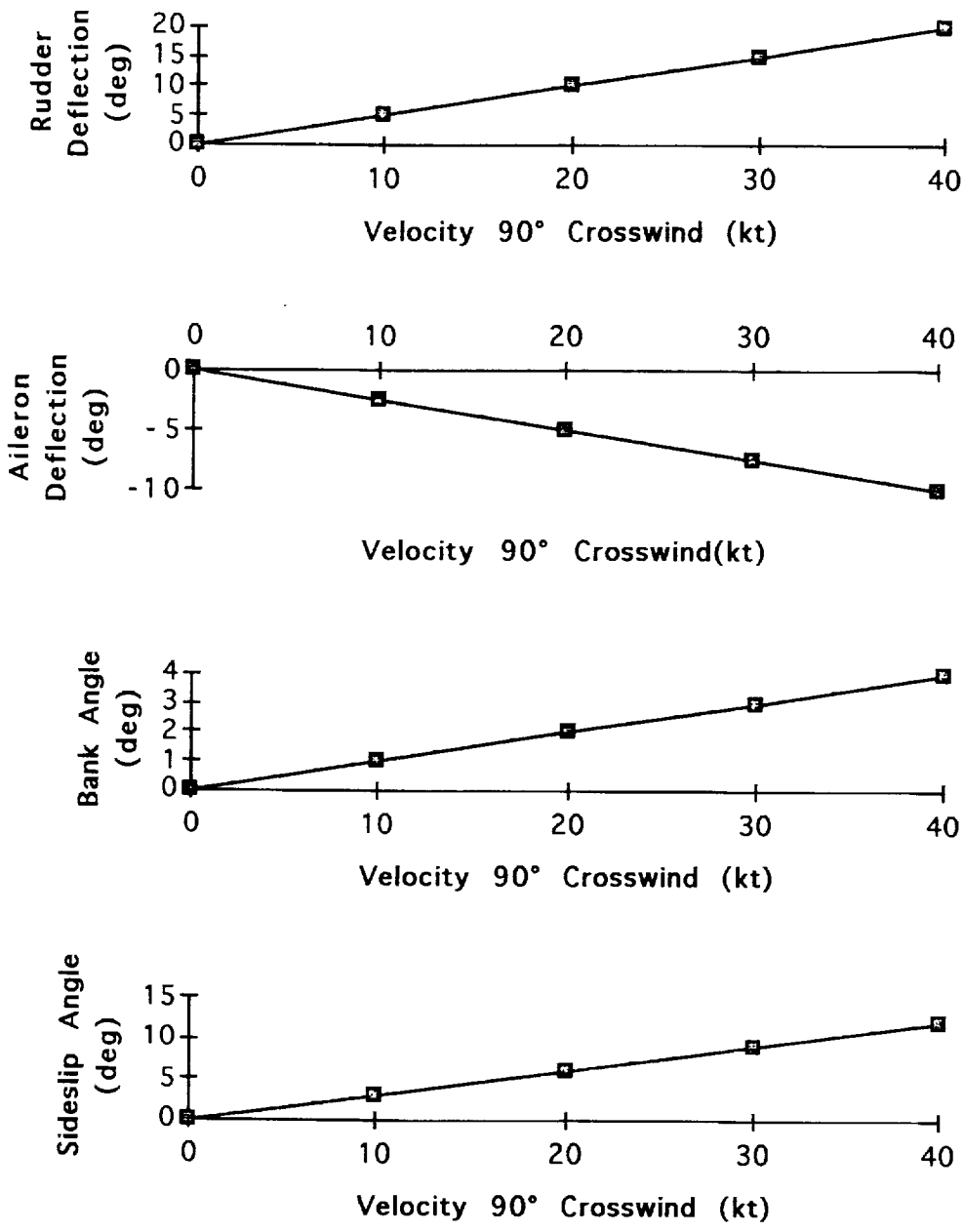

Figure 10.2 Crosswind Landing Characteristics

Roll control capability is a problem area for large multibody aircraft for the following reasons: roll inertia is large due to body spanwise spacing, the bodies placed out along the span cut into wing area which

would other wise be available for positioning control surfaces, such as ailerons or spoilers, and roll control specifications presently available are insufficient and impractical for very large aircraft.

It is obvious that roll control becomes increasingly difficult with fuselages located off the aircraft centerline. Predicting exactly where the cutoff should be is not easily done. MilSpec 87858B quantifies roll capability by specifying the time required to bank 30 degrees. For level 1, the desired normal capability, the time requirement is 2.7 seconds (Ref.25). The specification allows the time to increase to 3.2 and then 4.0 seconds for level 2 and 3, where level 3 is being able to land safely (Ref.25). The revised version of the specification 87885C allows the time to increase to 6.0 seconds for level 3 (Ref.25). The Ostrich does not meet this requirement, but neither does the Lockheed C-5, and the C-5 is still judged to have good flying qualities (Ref. 14).

A different approach to establishing a required level of roll capability is to perform the true mission of the aircraft on a flight simulator, with a pilot in the loop. During the Lockheed C-5 development, a lateral offset maneuver on landing approach was used as an evaluation task. However this is beyond the scope of this report and is only suggested as an alternative method to establishing a required level of roll capability (Ref. 14).

11.0 SYSTEMS

11.1 Fuel System

The fuel system of the Ostrich is shown in Figure 11.1. The main fuel bays are located in the wing with six independent fuel tanks supplying fuel to its associated engine with the capability of transfer to other engines. Each of the two inboard tanks are divided into three compartments called aft, forward, and feed compartments. As fuel is used, the remaining fuel supply moves forward of the spanwise bulkhead and then to the forward feed compartments. Each outboard tank is divided into the inboard, outboard, and feed compartments. As fuel is used, the remaining fuel is automatically moved toward the feed compartment for wing load alleviation. Both main bays contain a total volume sufficient enough to cover the design range of the airplane. Center auxiliary tanks are located in wing sections between the outer fuselages and the center fuselage. No fuel bays are located in the wing box within each fuselage. Dry bays and fire walls are also located behind each engine to separate fuel tanks from vital areas.

The fuel pumps are located such that refueling/defueling can be done from two stations located on the right wheel pod of the right fuselage and the left wheel pod of the left fuselage for easy access. There are also two stations located on the underside of the wing should the need arise for other fueling access. There will be two fuel pumps in each tank, with no two from the same tank being run by the same electrical source. All fuel pumps are dimensioned to supply 1.5 times the maximum required fuel flow by the engines as required for optimum design (Ref. 22).

A fuel venting system is also utilized to prevent excessive pressurization in the tanks and to maintain air pressure for the ram air

turbine while in flight. Surge tanks are also located at the end of each main fuel bay to collect and condense excess fuel vapor before exiting the overboard fuel vents. A fuel jettison system is also integrated into the management system for emergency landings (Ref. 22).

FOLDOUT FRAME

THE OSTRICH

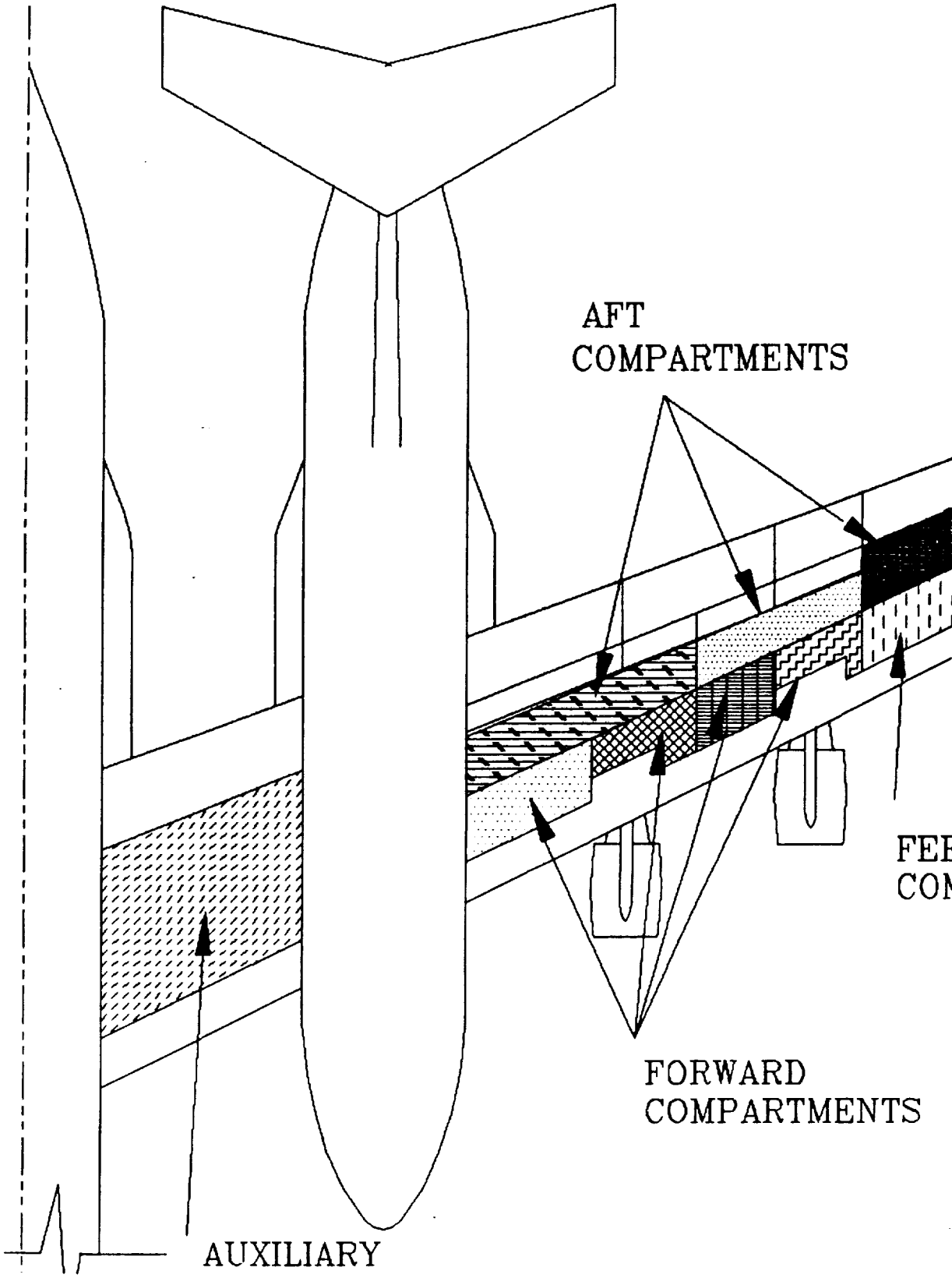

Figure 11.1 Fuel System for The Ostrich

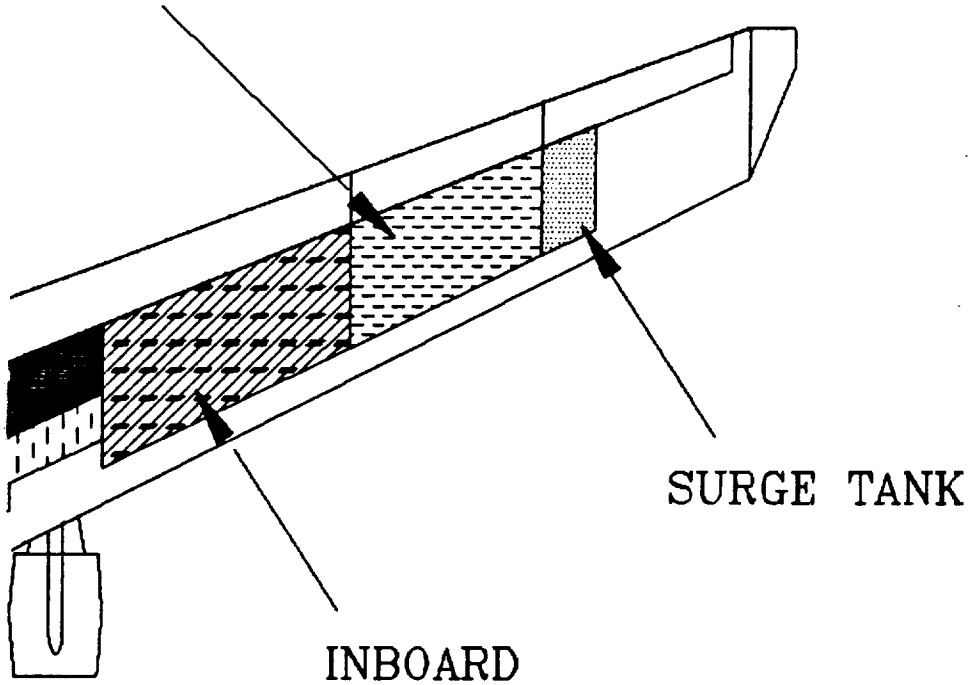

:D
/PARTMENT

11.2 Hydraulic System

The hydraulic system schematic of the Ostrich is shown in Figure 11.2. Six independent hydraulic systems, each with a primary and secondary pump, are required for safe flight operations. An advanced 8,000 psi system is incorporated for reduced weight and installed volume as compared to the standard bulkier 3,000 psi system. In case of power failure, there is a backup system available. Accumulators are provided for short duration hydraulic pressure, such as lowering landing gear. An auxiliary power unit (APU) and ram air turbine (RAT) located in the landing gear pods of the outer fuselages are also available to provide long duration emergency standby power to operate flight controls (Ref. 12).

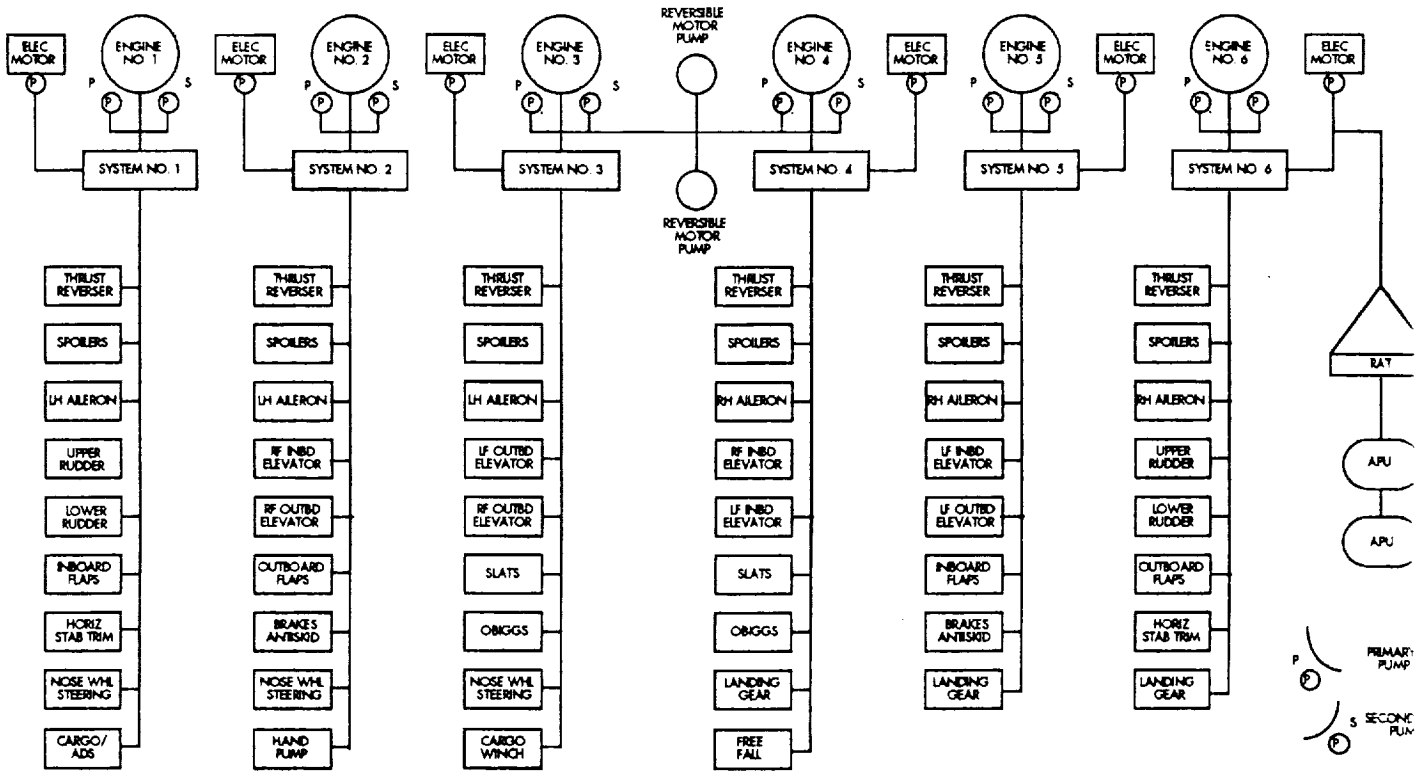

Figure 11.2 Hydraulic System Block Diagram for the Ostrich

11.3 Electrical System

A schematic of the electrical system of the Ostrich is shown in Figure 11.3. Electrical power will be used to power such systems as the internal and external lighting, flight instruments and avionics, flight control actuators, fuel pumps, and engine starting. Primary power will be supplied by AC generators driven by each engine. Their power will be fed to AC buses and to transformer/rectifier systems to derive DC power. Standby power will be supplied by the auxiliary power units (APU) and stored battery units. To allow for six independent electrical sub-systems, each engine will power a separate electrical generator bus. The APUs and

battery unit will be connected to each generator bus. The battery unit will also supply power to the APU starter.

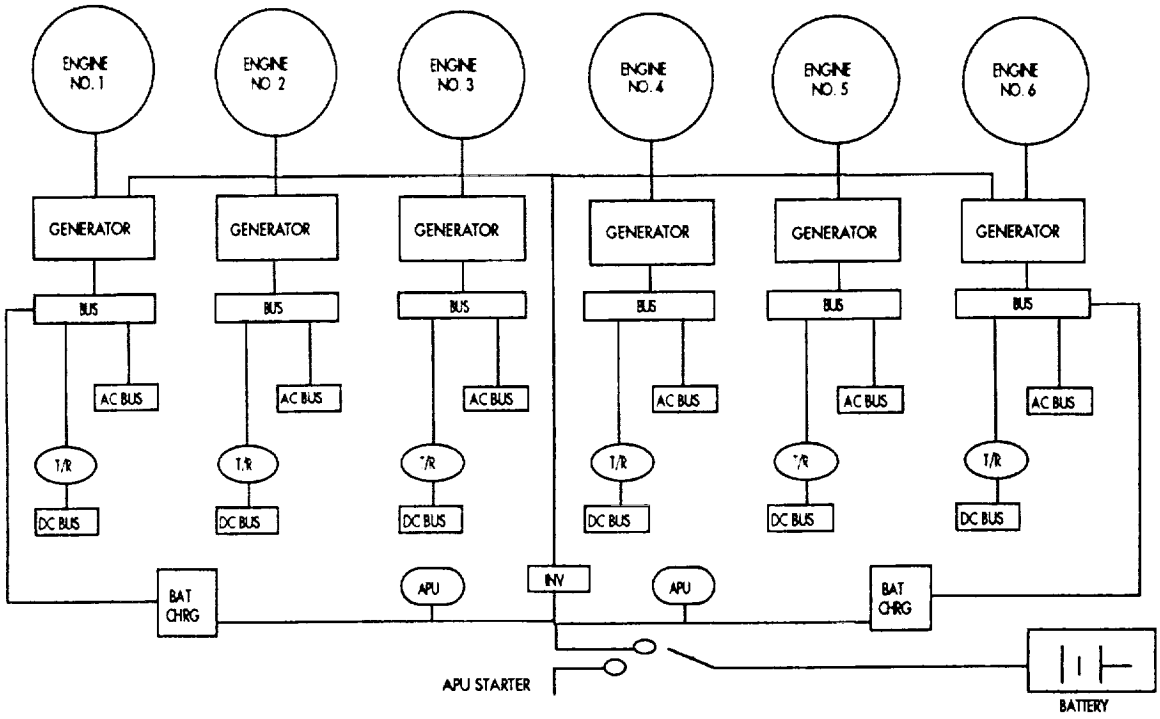

Figure 11.3 Electrical System Schematic for the Ostrich

11.4 Environmental Control Systems

11.4.1 Pressurization System

The constant inflow of conditioned air into the fuselage is released through the pressurization system outflow valve at a rate which maintains the pressurization schedule for each flight mission. Dual automatic systems are installed to maintain a sea-level cabin pressure up to 17,000 feet and an 8,000 foot cabin pressure at an aircraft altitude of 35,000 feet. Standby controls in each system permit depressurization in the cargo bays, separate of the passenger areas, at any altitude for high altitude cargo drops. An electrical manual control serves as backup to the dual system.

11.4.2 Pneumatic System

A pneumatic system for cabin pressurization will automatically control internal pressure in each fuselage equal to that at 8,000 feet. This system will contain fail safe mechanisms to prevent adverse pressure conditions. The pneumatic system also provides ice protection on the wing and the horizontal stabilizers. Cross engine starting will also be incorporated so that any engine can be started with another running engine.

11.4.3 Oxygen System

An oxygen system for flight at high altitudes will be provided using liquid oxygen converters. This system allows for weight and volume savings. Crew oxygen systems will incorporate a gaseous source. Individual oxygen masks will also be deployed to passengers in case of emergency. For the center fuselage, the general flow of air starts in the passenger area moving laterally and into the cargo area, and finally to the rear of the fuselage for exiting. The passenger and cargo area may be broken into separate temperature control zones should the need arise, for cases such as air drops. The outboard fuselages have similar airflow paths minus the temperature control zone for a passenger area. Accommodating oxygen systems for the load masters in each of the three cargo areas will also be available.

The ratio of recirculated air to fresh air in the passenger cabin will be maintained at around 2 to 1. The flight deck will receive air at a typical 20 cubic feet per minute per crew member and the passenger area will receive a sufficient level of 15 cubic feet per minute per passenger. Due to the critical heating levels involved with the electronic/electrical equipment racks and avionics, separate cooling will be supplied to keep them at

adequate temperatures. Separate ventilation of the air from the galley and lavatories will be adequately exhausted from the rest of the aircraft.

11.4.4 Water and Waste System

The water system will be pressurized with air from the pneumatic system. An electric heater will provide warm water to the washbasin in each toilet and also to the galley. Waste water from the toilets and galley is primarily discharged into waste tanks but also can be discharged directly overboard through electrically heated drains. The heating of these drains resists the formation of ice that could break off and cause aircraft problems.

The waste system is self contained and incorporates waste tanks (collector tanks) and flushing units which mix the waste with chemicals contained in the flushing liquid. Blowers are also incorporated to avoid any lingering odors should problems occur in the ventilation.

12.0 COST ANALYSIS

12.1 Airplane Estimated Price

The Ostrich has an airplane estimated price, AEP, of $1.2 billion for a 100 unit production. Figure 12.1 shows that the AEP is greatly dependent on the production quantity during the program.

12.2 Life Cycle Cost Breakdown

The cost analysis of the Ostrich was calculated by using the methods of Ref. 25 and Ref. 16. The following cost constraints were used:

- 15 year operational cycle
- 1993 dollars
- Fuel cost of $0.60 per gallon
- 700 flight hours per year utilization rate
- 100 unit production quantity during the program

The life cycle cost (LCC) includes the entire cost of the aircraft from planning and conceptual design to the time the aircraft is disposed of. The LCC can be broken down into four major areas:

1) research, development, test and evaluation cost (CRDTE)
2) acquisition cost (CACQ) including manufacturing cost;
3) operating cost (COPS)
4) disposal cost (CDISP)

The total LCC of this aircraft has been estimated to be $162 billion. The breakdown of this cost is shown in Figure 12.2.

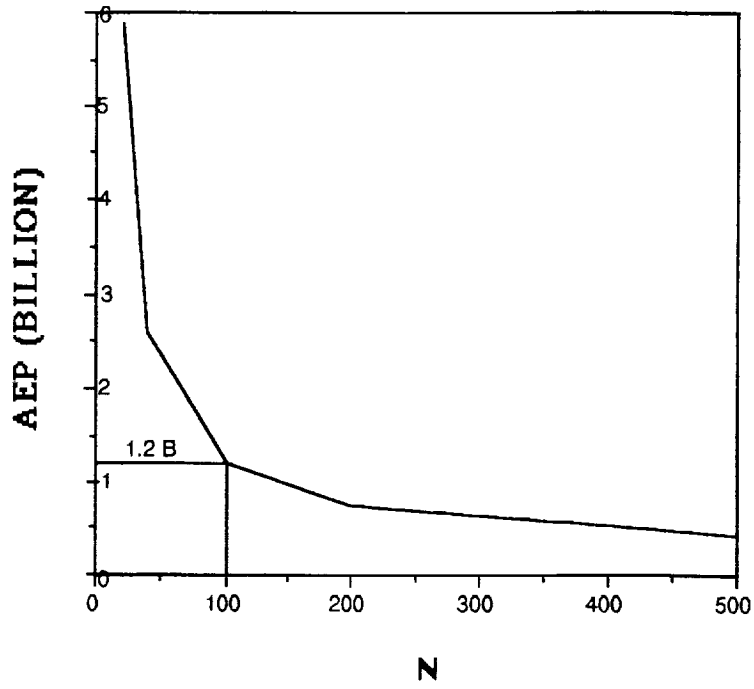

Figure 12.1 Airplane Estimated Cost per Unit vs No. Produced for the Ostrich

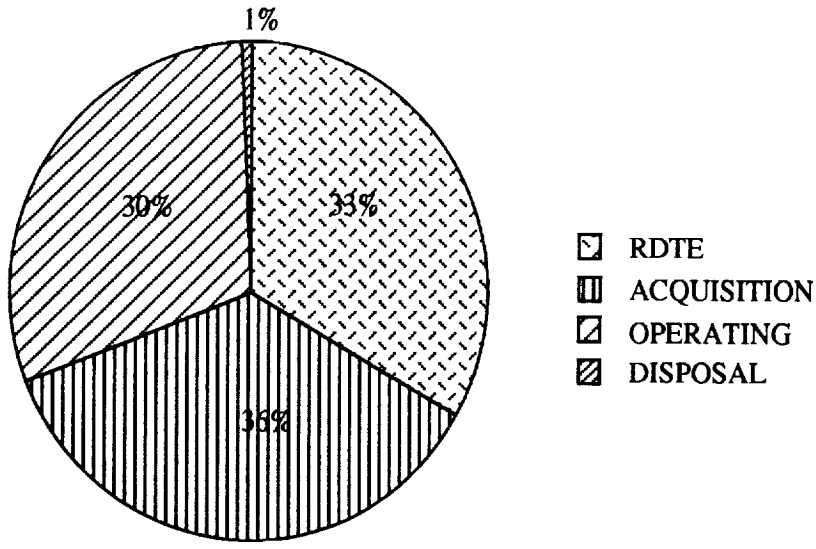

Figure 12.2 Life Cycle Cost for the Ostrich

The LCC of the Ostrich, which is composed of 56% graphite/epoxy, was compared to an aluminum aircraft. The aluminum aircraft was sized to accomplish identical mission requirements, providing comparisons based on equal airlift capabilities. The cost analysis of these two aircraft show that the operating cost of the aluminum aircraft is 20% greater and the LCC is 2% greater than that of the graphite/epoxy aircraft (Figure 20.3). This is primarily due to the reduction in weight resulting from the use of composites (Ref. 10). However, the AEP and the acquisition cost of the graphite/epoxy aircraft are 9% and 10% greater than that of the aluminum aircraft, respectively.

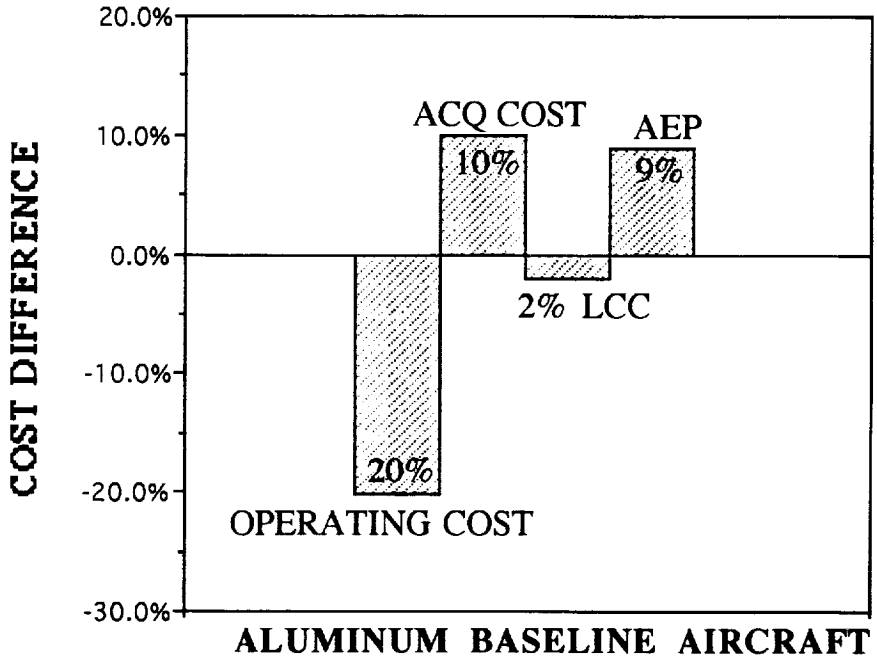

Figure 12.3 Cost Comparison Between Aluminum and Graphite for the Ostrich

13.0 CONCLUSION & RECOMMENDATIONS

Studies have shown an increased need for a global range military transport capable of carrying a large payload to anywhere in the world without ground support. The Ostrich is a solution to this problem.

The Ostrich has been designed as an aircraft that can be readily achieved by the year 2015. The unusually low specific fuel consumption was found to be within reach by 2010 and the propulsion systems currently satisfy the thrust requirements. Current trends show that composite materials will be used in primary structures in the near future and by utilizing existing technologies the cost of the aircraft can be kept to a minimum.

The Ostrich is an innovative approach to the problem deserving further investigation. Some of the areas which need to be studied further include LFC to obtain high lift to drag ratios, the use of all composites in primary structures, and the advantages and disadvantages of multibody configurations.

14.0 REFERENCES

1. AIAA/General Dynamics Corporation, Undergraduate Team Aircraft Design Competition (RFP), AIAA Student Programs, Washington D.C., 1992.

2. Anderson, John D., Introduction to Flight, McGraw-Hill Inc., New York, 1989.

3. Bauer, F., Supercritical Wing Sections II: A Handbook, Springer-Verlag, New York, 1975.

4. Currey, Norman S., Aircraft Landing Gear Design: Principles and Practices, American Institute of Aeronautics and Astronautics, Washington D.C., 1988.

5. Henemann, E. and Rausa, R., Aircraft Design, K.E. Van Every, The Nautical & Aviation Co. of America Inc., 1985.

6. Hoak, D.E. and Ellison, D.E. et al; USAF Stability and Control Datcom, Flight Control Division, Air Force Flight Dynamics Lab, Wright Patterson A.F.B., Ohio, 1992 edition.

7. Hoskin, B.C. and Baker, A.A., Composite Materials for Aircraft Structures, American Institute of Aeronautics and Astronautics, New York, NY, 1986.

8. Kandebo, S., GE 90 Program Moves Into High Gear , Aviation Week, McGraw-Hill, April 19,1993.

9. Lambert, M., Jane's All the World's Aircraft, Jane's Information Group Limited, Sentinel House, Virginia, 1991-92 edition.

10. Lang, R.H. and Moore, J.W., Application of Composite Materials and New Design Concepts for Future Transport Aircraft , International Council Of Aeronautical Sciences Procedings, American Institute of Aeronautics and Astronautics, New York, NY, 1982.

11. Lang, R.H., Design Integration of Laminar Flow Control for Transport Aircraft , American Institute of Aeronautics and Astronautics, New York, NY, 1983.

12. McDonnel Douglas, USAF/McDonnell Douglas C-17 Technical Description, Mcdonnell Douglas Corporation, Long Beach, CA.

13. Montoya, L.C., Flechner, S.G., and Jacobs, P.F., Effect of Winglets on a First-Generation Jet Transport Wing , NASA D-8474, July 1977.

14. NASA Langley Research Center, Multibody Aircraft Study Volume I, NASA, Hampton, Virginia, 1982.

15. NASA Langley Research Center, Multibody Aircraft Study Volume II, NASA, Hampton, Virginia, 1982.

16. Niu, Michael C.Y., Composite Airframe Structures , Conmilit Press Ltd., Hong Kong, 1992.

17. Preston, O.W., An Improved Method for Determining Aircraft Flexible Pavement Requirements, McDonnell Douglas, 1991.

18. Raymer, Daniel P., Aircraft Design: A Conceptual Approach , AIAA,Washington D.C., 1989.

19. Roskam, J., Airplane Design: Part I, Preliminary Sizing of Airplanes, Roskam Aviation and Engineering Corporation, Ottwa, Kansas, 1987.

20. Roskam, J., Airplane Design: Part II, Preliminary Configuration Design and Integration of the Propulsion System, Roskam Aviation and Engineering Corporation, Ottwa, Kansas, 1987.

21. Roskam, J., Airplane Design: Part III, Layout Design of Cockpit, Fuselage, Wing and Empennage: Cutaways and Inboard Profiles , Roskam Aviation and Engineering Corporation, Ottwa, Kansas, 1987.

22. Roskam, J., Airplane Design: Part IV, Layout Design of Landing Gear Systems, Roskam Aviation and Engineering Corporation, Ottwa, Kansas, 1987.

23. Roskam, J., Airplane Design: Part V, Component Weight Estimation,Roskam Aviation and Engineering Corporation, Ottwa, Kansas, 1987.

24. Roskam, J., Airplane Design: Part VI, Preliminary Calculation of Aerodynamic, Thrust and Power Characteristics , Roskam Aviation and Engineering Corporation, Ottwa, Kansas, 1987.

25. Roskam, J., Airplane Design: Part VII, Detrmination of Stability, Control and Performance Characteristics: Far and Military Requirements, Roskam Aviation and Engineering Corporation, Ottwa, Kansas, 1987.

26. Roskam, J., Airplane Design: Part VIII, Airplane Cost Estimation and Optimization: Design, Development Manufacturing and Operating, Roskam Aviation and Engineering Corporation, Ottwa, Kansas, 1987.

27. Roskam, J., Advance Aircraft Analysis Program, v.1.4 , Design Analysis & Research Corporation.

28. Taylor, M., Encyclopedia of Modern Military Aircraft , W.H. Smith Publishers, Inc., New York, NY, 1987.